JAERI-M
89-041

ANALYSIS OF THE WIND DATA AND ESTIMATION OF THE RESULTANT DOSES FROM THE SUPERSONIC ANEMOMETER

(A COMPARISON STUDY OF THE SUPERSONIC AND PROPELLER WIND DATA)

April 1989

Shze Jer HU *, Hiroshi KATAGIRI and Hideo KOBAYASHI

日本原子力研究所
Japan Atomic Energy Research Institute

JAERI-Mレポートは，日本原子力研究所が不定期に公刊している研究報告書です。
入手の問合わせは，日本原子力研究所技術情報部情報資料課（〒319－11茨城県那珂郡東海村）あて，お申しこしください。なお，このほかに財団法人原子力弘済会資料センター（〒319-11茨城県那珂郡東海村日本原子力研究所内）で複写による実費頒布をおこなっております。

JAERI-M reports are issued irregularly.
Inquiries about availability of the reports should be addressed to Information Division, Department of Technical Information, Japan Atomic Energy Research Institute, Tokai-mura, Naka-gun, Ibaraki-ken 319-11, Japan.

編集兼発行　日本原子力研究所
印　　刷　日立高速印刷株式会社

Analysis of the Wind Data and Estimation of the Resultant Doses from the Supersonic Anemometer (A Comparison Study of the Supersonic and Propeller Wind Data)

Shze Jer HU*, Hiroshi KATAGIRI and Hideo KOBAYASHI

Department of Health Physics
Tokai Research Establishment
Japan Atomic Energy Research Institute
Tokai-mura, Naka-gun, Ibaraki-ken

(Received March 10, 1989)

Statistical analyses and comparisons of the wind data obtained by the propeller and supersonic anemometers for the year of 1987 in Japan Atomic Energy Research Institute, Tokai Establishment were performed.

The resultant average air concentrations and ground level external γ exposure rates due to the radioactive releases for the normal operation of a nuclear power plant are over-estimated when calculated using the properller wind data. The difference is due to the influence of low wind speeds.

If the frequencies of low wind speed are large, wind data observed by the supersonic, which could measure even low wind speed more precisely then the propeller, should be used in the atmospheric dispersion analysis to yield a more accurate and realistic estimation of the air concentration and ground level external γ exposure rate.

The analysis also shows that the adult thyroid exposure dose of the postulated accident is sufficiently accurate and valid when estimated basing on the contributions of individual iodine nuclides without considering their decay and using the supersonic wind data without having to modify the assumed mean wind speed of the calm. For the external γ whole body exposure of the postulated accident, accurate and realistic

---

* Universiti Sains Malaysia

estimation should base on the contributions of individual radionuclides with their decay considered and use the supersonic wind data for atmospheric dispersion analysis.

Keywords: Supersonic Anemometer, Propeller Anemometer, Comparison, Wind Data, Air Concentration, External γ Exposure, Thyroid Exposure Dose, Whole Body Exposure, Decay

超音波型風向風速計による風速データの解析と線量評価
（超音波型とプロペラ型風向風速計による風速データの比較）

日本原子力研究所東海研究所保健物理部
Shze Jer HU*・片桐　浩・小林　秀雄

（1989年3月10日受理）

東海研究所気象観測塔に設置してある超音波風向風速計の特性をプロペラ型風向風速計のものと比較するために1987年のデータについて統計解析を行うとともに，両データを用いて被ばく線量の評価を行った。被ばく線量の評価には，ＮＵＣＥＦの放出量を参考に用いた。その結果，平常時における放射性物質の連続放出による年平均空気中放射能濃度と年平均γ線線量は，プロペラ型風向風速計による気象データを用いた方が，低風速域で風速が少なめに観測されるので，やや高い結果になった。また，事故時における空気中放射能濃度，γ線線量について，スタックと被ばく評価地点間における放射性よう素及び希ガスの核種毎の物理的減衰を考慮した場合の線量への影響についても評価した。

東海研究所：〒319-11 茨城県那珂郡東海村白方字白根2－4
＊　マレーシア科学大学

Contents

目　　次

1. Introduction

The atmosphere is an important pathway of gaseous nuclides relased from a nuclear power plant to the environment and thereby to man. Radioactive materials released to the atmosphere will be transported downwind and dispersed by normal atmospheric mixing processes. As the activity disperses, members of the public are irradiated internally owing to the inhalation of activity and externally by β- and γ-radiation from the plume. Thus adequate information about this pathway is necessary to estimate the dispersion of the radioactive releases to the population in the region and to assess the radiological impact on man.

Meteorological information is needed to determine the impact of short- or long-term routine radioactive releases on the environment during the routine operation of a nuclear power plant. Knowledge of meteorological conditions also enables appropriate countermeasures to be taken after an accidental release. Meteorological variables used in the dispersion calculation and their statistical analysis give the probability distribution of concentration of radioactive materials released from the plant. Thus the precision, nature and scope of the meteorological data should be compatible with the methods and models in which they are used for evaluating the radiological impact on the environment. The collected data should adequately represent local meteorological conditions. To understand the atmospheric behavior at the site completely, it is necessary to select correctly the position of the equipment and to obtain through the instruments a good representation of the whole field of the wind at least up to the height of possible releases.

In the Japan Atomic Energy Research Institute (JAERI), the method of the meteorological observation and the analysis on the statistic of the observed data and the atmospheric diffusion for normal operation and postulated accident of a nuclear power plant follow the meteorological guide of the Japan Atomic Energy Safety Commission[1]. The items of the observation consist of wind speed, wind direction, solar radiation, net radiation, precipitation and the vertical temperature gradients, etc. Other than the vertical temperature gradient and precipitation, ten minutes average data before every hour on the hour are representatively used for the analysis. For temperature gradient, instantaneous value of every hour is used while for precipitation, one hour accumulated value before every hour is used. The instruments, their characteristics and their mounting heights are shown

in Table 1.1. Definitions and units of the statistical items are as given in Table 1.2. The atmospheric stability is classified by Pasquill-Maede[2] method using the representative surface wind speed, insolation or net radiation of the site (Table 1.3).

The wind directions and wind speeds in JAERI were measured using only wind mill type anemometer (vane properller type) before 1987. Although this type of propeller anemometer is very commonly used all over the world and long term experience has shown that it is operationally reliable, it has the disadvantage of not giving accurate reading at low wind speed. Since 1987, supersonic anemometers were also installed in the JAERI meteorological tower for wind measurement. Both the propeller and supersonic anemometers are periodically calibrated by the Japan Weather Association according to its technical manual. The supersonic anemometers, however, can provide precise wind speed down to as low as 0.01 m/s. (By the specification of supersonic anemometer maker, it can measure as low as 0.01 m/s.) Thus the availability of the more accurate wind speeds and wind directions from the supersonic anemometers provides a better representations of the wind field especially under calm condition, defined when wind speed by propeller is less than 0.5 m/s. A more realistic and accurate estimation of the atmospheric dispersion of the radioactive releases from the nuclear power plant can also be obtained.

Analyses were carried out in the present study to compare the one year wind data obtained in 1987 by the two different types of anemometer. The purpose is to identify whether significant difference occurs between the two sets of meteorological data and to investigate how the difference might affect the average air concentrations and γ exposure rates due to the radioactive releases from the nuclear power plant. The average air concentrations and exposure rates due to the normal operation of research reactor were estimated and compared using the supersonic and propeller wind data sets. The effect of the calm condition on these calculations was also studied by modifying the wind speed of calm to be less than 0.1 m/s using supersonic anemometer. A comparison study using the two different sets of wind data was also performed for the postulated accident with 1 hour effective release time. For the postulated accident study, the adult thyroid exposure doses due to the iodine nuclides and the external γ whole body exposures due to the Xe, Kr and iodine nuclides were estimated.

2. Analysis of the wind data obtained by propeller and supersonic anemometers

Radioactive materials released to the atmosphere will be transported downwind and dispersed by normal atmospheric mixing process. As the diffusion of the released materials depends very much on the wind speed, wind direction and atmospheric stability, we begin our study by the statistical analysis of the wind data obtained by supersonic and propeller type anemometers for the year of 1987.

2.1 Comparison of the monthly and yearly averages of wind speeds and percentage of calm

The monthly and yearly statistical averages of the meteorological data obtained by the supersonic and propeller anemometers are shown in Table 2.1a and Table 2.1b respectively. Other than the wind speeds and calm, the values of all the other items are the same in both tables.

All monthly and yearly wind speed averages obtained by supersonic anemometer at 10m, 20m and 40m height are higher than those obtained by propeller anemometer. The yearly wind speed averages of the supersonic data at 10m, 20m and 40m height are 2.1 m/s, 3.0 m/s and 4.1 m/s respectively. In the case of the propeller data, their values are 1.8 m/s, 2.7 m/s and 3.7 m/s respectively. These results can be substantiated by the monthly and yearly calm percentage obtained by the two types of anemometer. Here, all the calm percentages obtained by propeller anemometer at the three different altitudes are of higher value than those obtained by supersonic anemometer. As the calm is defined to be the condition when wind speed is less than 0.5 m/s, the higher percentage of calm implies lower average wind speed. The yearly averages of the calm percentage for propeller data at 10m, 20m and 40m are 15%, 4% and 2.2% respectively. Those of supersonics are 2.6%, 0.8% and 0.6% respectively. These results also show that calm is less likely to occur at higher altitude. As precise and accurate wind measurement can be obtained through the supersonic anemometer especially at low wind speed, we conclude that wind speed readings obtained through propeller anemometer are lower than the actual wind speeds. Owing to the mechanical characteristic of the vane propeller anemometer, the inaccurracy of the wind speeds measured by the propeller anemometer is especially prominent at low wind speed. For wind speed greater than 1 m/s, the discrepancy is less significant. The correlation between the 10m and 40m height hourly average wind speed readings

obtained by propeller anemometers and the corresponding wind speed readings obtained by supersonic anemometers is shown as equation (1).

$$WSs = 0.96WSp + 0.52 \quad (1)$$

and is shown in Fig. 2.1.

Where WSs is the wind speed obtained through supersonic anemometer and WSp is the wind speed obtained through propeller anemometer.

The total number of wind speed data used for the correlation is 17201. This result shows that all wind speeds obtained through propeller anemometers are approximately 0.5 m/s less than the actual wind speeds if we assume the readings obtained through supersonic anemometers represent the actual wind speed.

The annual percentage frequency distribution of wind direction obtained through supersonic and propeller anemometers are shown in Table 2.2a and 2.2b respectively. The values obtained through the two different types of anemometer vary for all the 16 directions at the three different altitudes. Here, as expected, the difference is again more prominent for readings obtained at the lowest altitude i.e. 10m height, owing to the more frequent occurrence of calm.

2.2 Comparison of the annual percentage frequency distribution of stability category

An important factor in the Pasquill-Maede's classification of atmospheric stability is wind speed. It is thus interesting and useful to see how the annual percentage frequency distribution of stability category varies as a consequence of using ths two different sets of wind speed data obtained at 10m height. Table 2.3a shows the annual percentage frequency distribution of stability category obtained through supersonic and propeller anemometers. On combining categories A-B and B as category B, categories B-C and C as category C, categories C-D, D_1 and D_2 as category D and categories F and G as category F, we obtained Table 2.3b. Table 2.3b shows that percehtage of the categories A, B and F from the supersonic data have decreased with respect to those from the propeller data. As for categories C, D and E, the percentages from the supersonic data have increased with respect to those from the propeller data. These results are logical because our correlation study shows that all wind speeds less than or equal to 2 m/s measured by propeller anemometer are lower than those measured through supersonic anemometer. The difference in the wind speeds measured by the two types of anemometers is less significant when wind speed

is higher than 2 m/s. Since the values of the insolation and net radiation (of the stability classification table) for the two sets of wind speeds data are the same, it is logical that the percentages of categories A, B and F from the supersonic data should decrease. This is because the number of wind speeds with value less than 2 m/s from the supersonic wind data set for these categories is less compared to that from the propeller wind data set. The higher wind speed values obtained through supersonic anemometer also explains why the percentages of catagories C, D and E of the supersonic data set increase. The increase in category E of the supersonic data set is due to the decrease of category F with wind speed $u < 2$ m/s. While the increase of category C is mainly due to the decrease in category B with wind speed $u <$ 2 m/s. As for category D, its increase comes mainly from category E with wind speed 2 m/s $\leq u < 3$ m/s. However, the annual percentage frequency distribution of all the categories from the two different set of wind data on the whole differ by less than 2%.

2.3 Sum of the inverse of wind speeds and mean of the inverse of wind speeds for every wind direction and stability

In the analysis of the atmospheric diffusion of radionuclide released from the routine operation of nuclear plants, the hourly meteorological data are processed statistically for the sum of the inverse of wind speed and the mean of the inverse of wind speed for every wind direction and stability[1].

The sum of the inverse of wind speed $S_{d,s}$ for wind direction d and atmospheric stability s is calculated by summing the contribution of the windy condition ${}_{w}S_{d,s}$ and calm condition ${}_{c}S_{d,s}$, which is expressed in equation (2).

$$S_{d,s} = {}_{w}S_{d,s} + {}_{c}S_{d,s} \tag{2}$$

where $${}_{w}S_{d,s} = \sum_{i=1}^{N} \frac{{}_{d,s}\delta_i}{U_i} \tag{3}$$

N : the number of data observed

U_i : wind speed at time i, (m/s)

${}_{d,s}\delta_i$ is 1 when the wind direction is d and the atmospheric stability is s, otherwise it is 0

and $${}_{c}S_{d,s} = \frac{{}_{c}N_{d,s}}{{}_{c}U} \tag{4}$$

${}_{c}U$ is the assumed wind speed on calm condition (= 0.5 m/s)

${}_{c}N_{d,s}$ is the number of occurrence of calm condition at wind direction d and atmospheric stability s and is given by equation (5).

$$ {}_{c}N_{d,s} = \frac{N'_d}{\sum_{d=1}^{16} N'_d} \, {}_{c}N_s \qquad (5) $$

N'_d is the frequency of wind direction d with wind speed from 0.5 m/s to 2 m/s

${}_{c}N_s$ is the frequency of stability s on calm condition

The mean of the inverse of wind speed $\overline{S}_{d,s}$ for wind direction d and atmospheric s is calculated by equation (6).

$$ \overline{S}_{d,s} = \frac{S_{d,s}}{N_{d,s}} \qquad (6) $$

where $N_{d,s}$ is the total number of appearance of wind with direction d and atmospheric stability s.

Tables 2.4a and 2.4b are respectively the sum of the inverse of wind speed and the average of the inverse of wind speed for every wind direction and stability calculated by using the propeller data set obtained at 40m height. Tables 2.5a and 2.5b are the corresponding tables calculated using the supersonic data set at 40m height. A comparison of the total sum of the inverse wind speed from each wind direction of the propeller wind data with those of the corresponding directions of the supersonic wind data shows all the 16 directions of the propeller wind data have values greater than those from the corresponding directions of the supersonic wind data. This results is as expected because the higher wind speeds measured by the supersonic anemometer will yield a lower total sum of the inverse wind speed. Nonetheless this comparison is not too meaningful as it may not be so accurate owing to the fact that the frequency distributions of wind direction for a specific direction may not be the same from the two sets of wind data as a result of the statistics used in assigning the wind direction of the calm. The discrepancy can be seen when a similar comparison is made between the total sum of the inverse wind speed from each wind direction of the propeller data set obtained at the 10m height (Table 2.6a) and the corresponding value of the supersonic data set also obtained at 10m height (Table 2.7a). Thus no further similar comparison is made between the two different wind data sets. Since the mean of the inverse of wind speed for every wind direction and stability is calculated directly from the sum of the inverse of wind speed for every wind direction and stability, no comparison of the means of the inverse of wind speed from the two sets of wind data is made.

Tables 2.8a and 2.8b show the sum of the inverse of wind speed and the mean of the inverse of wind speed for every wind direction and stability respectively obtained by supersonic anemometer at 40m height when the assumed wind speed of the calm condition, $_{c}U$ is changed to 0.1 m/s. This analysis was carried out because the supersonic anemometer can measure accurately and precisely wind speed to as low as 0.01 m/s. It is interesting to investigate whether any difference will occur when the assumed wind speed of calm conditions, $_{c}U$ is changed from 0.5 m/s to 0.1 m/s except the propeller data. By changing the calm condition from $u < 0.5$ m/s to $u < 0.1$ m/s, the number of calm at each stability category will certainly decrease. Table 2.9 shows the number of calm occuring at each stability category for propeller data set and supersonic data set. In the case of the supersonic data set, the numbers of calm for both $u < 0.5$ m/s and $u < 0.1$ m/s conditions are shown. Because of the higher wind speed readings obtained by supersonic anemometer, the number of calm at each stability category from the supersonic data set at different height is much less than the corresponding number from the propeller data set. When the assumed wind speed of the calm condition is changed to 0.1 m/s, Table 2.9 shows that the number of calm in the supersonic data occurs only once each at 10m height and at 40m height. No calm occurs at all at 20m height. This mean that the total sum of the inverse wind speed for each stability category except categories C and E will be larger now after the assumed wind speed of the calm condition is changed to 0.1 m/s. No change occurs in categories C (where categories B-C and C are combined) and E because there is no calm in these two categories originally. A comparison of the last column of Tables 2.5a with that of Table 2.8a does verify this result. A similar comparison of the last column of Table 2.7a with that of Table 2.10a (both sets of data are at 10m height) also shows the same result. Thus the total sum of the inverse wind speed for each stability category is a better indicator to show the difference of the sum of the inverse wind speed obtained as compared to the total sum of the inverse wind speed for each direction.

3. Air concentration and γ exposure rate calculated using the propeller and supersonic wind data for normal operation

Air concentration

The sum of the inverse of wind speeds for every wind directions and

Tables 2.8a and 2.8b show the sum of the inverse of wind speed and the mean of the inverse of wind speed for every wind direction and stability respectively obtained by supersonic anemometer at 40m height when the assumed wind speed of the calm condition, $_cU$ is changed to 0.1 m/s. This analysis was carried out because the supersonic anemometer can measure accurately and precisely wind speed to as low as 0.01 m/s. It is interesting to investigate whether any difference will occur when the assumed wind speed of calm conditions, $_cU$ is changed from 0.5 m/s to 0.1 m/s except the propeller data. By changing the calm condition from $u < 0.5$ m/s to $u < 0.1$ m/s, the number of calm at each stability category will certainly decrease. Table 2.9 shows the number of calm occuring at each stability category for propeller data set and supersonic data set. In the case of the supersonic data set, the numbers of calm for both $u < 0.5$ m/s and $u < 0.1$ m/s conditions are shown. Because of the higher wind speed readings obtained by supersonic anemometer, the number of calm at each stability category from the supersonic data set at different height is much less than the corresponding number from the propeller data set. When the assumed wind speed of the calm condition is changed to 0.1 m/s, Table 2.9 shows that the number of calm in the supersonic data occurs only once each at 10m height and at 40m height. No calm occurs at all at 20m height. This mean that the total sum of the inverse wind speed for each stability category except categories C and E will be larger now after the assumed wind speed of the calm condition is changed to 0.1 m/s. No change occurs in categories C (where categories B-C and C are combined) and E because there is no calm in these two categories originally. A comparison of the last column of Tables 2.5a with that of Table 2.8a does verify this result. A similar comparison of the last column of Table 2.7a with that of Table 2.10a (both sets of data are at 10m height) also shows the same result. Thus the total sum of the inverse wind speed for each stability category is a better indicator to show the difference of the sum of the inverse wind speed obtained as compared to the total sum of the inverse wind speed for each direction.

3. Air concentration and γ exposure rate calculated using the propeller and supersonic wind data for normal operation

Air concentration

The sum of the inverse of wind speeds for every wind directions and

atmospheric stabilities and the frequency distribution of wind directions calculated using the wind speed data obtained at 40m height can now be used to estimate the air concentration and γ exposure rate due to the radionuclides released from the normal operation of nuclear power plant.

The equation used to calculate the air concentration $\chi(x,y,z)$ is the standard Gaussian plume equation equation (7).

$$\chi(x,y,z) = \frac{Q}{3600 \cdot 2\pi \cdot u \cdot \sigma_y \cdot \sigma_z} \exp\left[-\frac{\lambda}{u}x\right] \exp\left[-\frac{y^2}{2\sigma_y^2}\right] \left[\exp\left[-\frac{(Z-H)^2}{2\sigma_z^2}\right] + \exp\left[-\frac{(Z+H)^2}{2\sigma_z^2}\right]\right] \quad (7)$$

where $\chi(x,y,z)$ is the air concentration in Ci/m^3,

Q is the radionuclides release rate, (Ci/h)

u is the wind speed, (m/s)

σ_y and σ_z are the horizontal and vertical plume width as a function of downwind distance, (m)

H is the effective stack height (m) and

λ is the decay constant of the radionuclide (1/s)

The average air concentration of ground surface $\overline{\chi}(x,y)$ for a given point is then obtained by the equation (8).

$$\overline{\chi}(x,y) = \overline{\chi}_0(x,y) + \overline{\chi}_{-1}(x,y) + \overline{\chi}_{+1}(x,y) \quad (8)$$

where $\overline{\chi}_0$ is the average air concentration when the downwind is in the direction of the point (x,y),

$\overline{\chi}_{-1}$ and $\overline{\chi}_{+1}$ are the average air concentration when the downwind is in the neighbouring direction ($\pm$ 1) of the point (x,y).

For continuous radionuclide releases from the normal operation of the nuclear power plant,

$$\overline{\chi}_J = \frac{Q_c}{N_t} \sum_{S=A}^{F} S_{JS}\overline{\chi}_{JS} \quad (9)$$

where Q_c is the continuous release in Ci/h,

N_t is the total number of wind speed observed (8760),

S_{JS} is the sum of the inverse of wind speed for J direction and S stability, and

$\overline{\chi}_{JS}$ is the average air concentration when wind direction is J and stability is S.

External γ whole body exposure by submersion model

When a person is submerged in a radioactive gas, the skin and other organs of the body may be irradiated both by external irradiation and by internal irradiation from the gas absorbed into the body tissues. According to the submersion model[3], the exposure rate is proportional to air concentration and to the energy of the photon. From the average air concentration obtained, the yearly external γ whole body exposure, $D_{\gamma s}$ in mrem/y can be calculated by the submersion model using equation (10).

$$D_{\gamma s} = \frac{1}{2} K E_{\gamma} \chi \qquad (10)$$

where E_{γ} is effective γ energy in MeV/dis and

K is the conversion factor for external γ whole body exposure,

$1.15 \times 10^{10} \left(\frac{dis.m^3.mrem}{MeV.Ci.y} \right)$

Ground level external γ exposure by plume model

The ground level external γ exposure rate due to the radioactive plume is calculated by the following equation (11)[4].

$$D = K_1 K_2 E \mu_a \int_0^{\infty} \int_{-\infty}^{\infty} \int_0^{\infty} \frac{\beta(\mu r) e^{-\mu r}}{4\pi r^2} \chi(x',y',z') dx'dy'dz \qquad (11)$$

where D is the exposure rate at point (x,y,o), mrem/h

K_1 is the constant for converting the exposure to absorbed dose, 0.7 mrem/mR

K_2 is the constant for converting activity to exposure rate, 1.88×10^6 $\left(\frac{dis.m^3.mR}{MeV.Ci.h}\right)$

E is the effective energy of the photon, MeV/dis

μ_a and μ are the true and total linear absorption coefficient, m^{-1}

r is the distance in meter between the receptor and a volume element of the cloud

$\beta(\mu r)$ is the dose build-up factor calculated by[5]

$$\beta(\mu r) = 1 + \alpha(\mu r) + \beta(\mu r)^2 + \gamma(\mu r)^3 \qquad (12)$$

In this calculation, μ_a, μ, α, β and γ have values correspond to photon of 500 keV energy.

The yearly exposure at a given point, D in unit of mrem/y is calculated by equation (13).

$$D = \overline{D}_J + \overline{D}_{J-1} + \overline{D}_{J+1} \qquad (13)$$

where D_J, D_{J-1}, D_{J+1} are exposure at a given point due to radioactive clouds in downwind direction (J) and neighbouring direction (J-1, J+1).

For continuous radionuclides releases from the normal operation of the nuclear power plant,

$$D_J = \frac{Q_c}{N_t} \sum_{S=A}^{F} S_{JS} \overline{D}_{JS}$$

where Q_c is the continuous release rate in MeV Ci/h
(= 1MeV Ci/h) and
$\overline{D}_{JS}$ is the average exposure rate of the calculated point at wind direction J and atmospheric stability S.

3.1 Comparison of calculated average air concentrations

Table 3.1 shows the ground level external γ exposure rates $D_{\gamma S}$ and the average air concentrations $\overline{\chi}$ calculated at a distance of 1km due to the continuous release of radionuclides at 40m stack height. They are calculated for 16 downwind directions using the propeller or the supersonic (with calm conditions of $u < 0.5$ m/s and $u < 0.1$ m/s) wind data. Unit release of rare gases (i.e. 1MeV·Ci/h) and ^{131}I and ^{133}I (i.e. 1Ci/h) are used in the calculation. The plot of the average air concentration and the ground level external γ exposure rate for the 16 downwind directions are shown in Fig. 3.1 and Fig. 3.2 respectively.

The average air concentration calculated using supersonic wind data for most of the directions are generally lower than those calculated using propeller wind data. This result is as expected because the wind speeds measured by supersonic anemometer are generally higher compared to the values measured by propeller anemometer. Thus the sum of the inverse of wind speeds from the supersonic wind data being generally lower compared to the corresponding sum of the inverse of wind speeds from the propeller wind data will yield lower air concentrations for the supersonic data.

From Fig. 3.1, it is seen that the more prominent decreases occur at downwind directions SE, SSE, S, SSW and SW. In the S downwind direction because of the smaller sum of the inverse of wind speed, the decrease in the supersonic average air concentration is as high as 50%. The plots in Fig. 3.1 also show that the shapes of the 3 curves are rather similar. This is because not much difference occurs in the annual frequency distribution of wind direction between the two different sets of wind data at 40m height (Tables 2.2a and 2.2b). The little difference in the annual frequency distribution of the wind direction is due to the low influence of calm since the number of calm at 40m height is small (Table 2.9). Thus

with the majority of the measured wind speeds at higher speed, the wind directions measured using the two different anemometers are very similar. This explains why the curves have very similar shape.

γ exposure curves calculeted from the submersion model in Fig. 3.2 are identical in shape as those in Fig. 3.1. This is as expected since ground level external γ exposure rate is calculated directly from the average air concentration using the submersion model. Thus no comparison is made here concerning the ground level external γ exposure rates obtained for the 16 directions using the 2 different sets of wind data.

3.2 Comparison of the calculated γ exposure rates by Plume model

Table 3.2 shows the ground level external γ exposure rate, D_γ, due to the radioactive cloud calculated at a distance of 1 km due to the continuous release of radionuclides at 40m stack height. They are calculated for 16 directions using the propeller and the supersonic (two calm conditions of $u < 0.5$ m/s and $u < 0.1$ m/s are calculated for the supersonic.) wind data. Unit releases of rare gases, ^{131}I and ^{133}I are used in the calculation. The plot of the calculated values for the 16 directions are shown in Fig. 3.3.

From Fig. 3.3, it is again seen that the ground leve external γ exposure rates due to the radioactive cloud calculated using supersonic wind data of all the directions are generally lower than those calculated using propeller wind data. The overall shapes of the curves plotted using the two different wind data are similar because of the little influence from the calm at 40m height. The decrease in all the directions for the supersonic exposure rates are also rather similar to those of the supersonic average air concentrations. Here the more prominent decreases also occur at downwind directions ESE, SE,SSE, S, SSW and SW. The maximum decrease of the supersonic exposure rate which also occurs at S downwind direction is as high as 49%. Thus both the average air concentrations and the ground level external γ exposure rates due to the radioactive cloud are over-estimated when calculated using the wind data obtained by propeller anemometer. Although the estimated values using wind data obtained by propeller anemometer are more conservative, for a more accurate and relistic estimation of these calues for the normal operation of a nuclear power plant, supersonic anemometers are recommended to be used in the meteorological tower to measure as accurately as possible the exact wind speeds and wind directions especially when the wind speeds are low. This is especially critical when wind data are measured at the lower part of the meteorological tower where

the wind speed tends to be slower and only supersonic anemometer can give accurate measurement of wind speed to as low as 0.01 m/s.

3.3 Comparison of the calculated average air concentrations and γ exposure rates when the calm condition is modified

When the calm condition is modified by changing the assumed wind speed at calm condition from 0.5 m/s to 0.1 m/s, the calculated average air concentrations and the ground lever external γ exposure rates using the supersonic wind data obtained at 40m stack height (i.e. 40m stack height release) do not differ much from before (i.e. when $_{c}U$ = 0.5 m/s). Although their values are slightly higher in almost all the 16 downwind directions, they are not statistically different from those of $_{c}U$ = 0.5 m/s. This result is of course due to the fact that the number of calm of the 40m height supersonic wind data is small. Thus, in spite of the availability of the accurate and precise low wind data obtained by supersonic anemometer, the definition of calm (i.e. when u < 0.5 m/s, the frequency of wind direction is assumed to be the same as in the case of wind speed of between 0.5 m/s and 2.0 m/s, and the mean wind speed $_{c}U$ is assumed to be 0.5 m/s) for the statistical analysis is valid and requires no modification if the number of occurrence of low wind speeds (< 0.5 m/s) is low. However, if the number of occurrence of calm is large, the next section (Section 3.4) shows that a more accurate and realistic estimation of the average air concentration due to the normal operation of nuclear power plant can be obtained only if the exact low wind speeds and exact wind directions are used in the ststistical analysis of the sum of the inverse of wind speeds.

3.4 Average air concentrations calculated using 10 m wind data

To substantiate our earlier statement that the average air concentration and the ground level external γ exposure rates for normal nuclear power plant operation are over-estimated when calculated using the propeller wind data, we carried out further average air concentration estimation due to the release of radionuclides at 10m stack height using the 10m heiht wind data. Since the wind speeds at 10m height are much lower compared to those at 40m height, a greater number of calm will occur when measured using a propeller anemometer. The greater number of calm (Table 2.9) obtained by the propeller anemometer certainly has more prominent influence on the calculated average air concentrations.

The plots of the average air concentrations for the 16 directions at 1km distance from the release point using the 2 sets wind data are shown in Fig. 3.4. As expected, the average air concentrations calculated using supersonic wind data for all the directions are lower than those calculated using the propeller wind data. The more prominent decreases still occur at downwind directions SE, SSE, S, SSW and SW. Nonetheless, the magnitude of the decrease is much greater as compared to the corresponding decreases obtained using the 40m height wind data. The decrease in the estimated average air concentration at downwind directions S, SE, SSE and SSW are 72%, 64%, 55% and 45% respectively. This larger difference is due to the influence from the larger number of calm measured by the propeller anemometer, subsequently yielding a larger sum of the inverse of wind speeds. The influence of the larger number of calm can also be seen by the slight shift of the curve of the propeller with respect to the curve of the supersonic. This is because the frequency of the wind direction at calm condition is assigned to be the frequency of wind direction with wind speed from 0.5 m/s to 2 m/s. The larger number of calm from the propeller wind data will affect to a certain extent the directional distribution of the average air concentration estimated.

A comparison of the average air concentration estimated for the $u < 0.5$ m/s and $u < 0.1$ m/s calm conditions using the supersonic wind data at 10m height shows the difference that exists in all the directions being more significant when compared to the difference obtained between the two calm conditions for supersonic wind data at 40m height. The increase in the estimated average air concentration for land region is especially significant. The increase is due to the larger number of calm occuring at 10m wind data. By changing the assumed wind speed of the calm condition from 0.5 m/s to 0.1 m/s, the number of calm in the wind data will decrease (Table 2.9). This causes the sum of the inverse of wind speed for the latter calm condition where $u < 0.1$ m/s to be larger, thus yielding higher estimated average air concentrations.

When compared to the estimated average air concentration obtained using the propeller wind data, the values obtained for supersonic wind data with $u < 0.1$ m/s calm condition are still very much lower. This is because wind speeds with $u < 0.5$ m/s and $0.5 \text{ m/s} \leq u \leq 1$ m/s affect the estimated average air concentration differently. Although all supersonic wind speeds with values less than 0.5 m/s for the $u < 0.1$ m/s calm condition will now yield a larger sum of the inverse of wind speed compared to the corresponding wind

speeds of the propeller data (because the mean wind speed is now assumed to be 0.1 m/s), those supersonic wind speeds with values 0.5 m/s $\leq$ u $\leq$ 1 m/s will yield a smaller sum of the inverse of wind speeds compared to the corresponding wind speeds of the propeller data (because our earlier correlation study shows that all wind speeds $\leq$ 1 m/s obtained by propeller anemometer are approximately 0.5 m/s less than those obtained by supersonic anemometer). As the total number of calm at 10m height of the propeller data is very much larger than that of the supersonic data (column 8 and 9 of Table 2.9), it is clear that the majority of the wind speeds with value less than 0.5 m/s recorded by the propeller anemometer are actually greater than 0.5 m/s. Thus the latter contribution (i.e. wind speeds with 0.5 m/s $\leq$ u $\leq$ 1 m/s) to the sum of the inverse of wind speed has a greater effect in the estimated average air concentrations. This explains why in spite of the fact that the calm condition has been modified to u < 0.1 m/s for the supersonic wind data, the average air concentrations obtained from the supersonic wind data are still much lower compared to those obtained from the propeller wind data.

4. Analysis of atmospheric diffusion at the postulated accident using the propeller and supersonic wind data

In this section we investigate the effect of the propeller and supersonic wind data on the analysis of atmospheric diffusion at the postulated accident.

The air concentration of radionuclides released for the dose calculation at postulated accident is calculated using downwind concentration per unit release multiplied by the total release during the accident. We consider here only the short time release (1 hour effective release time), where by the relative air concentration χ/Q in h/m^3 is given equation (15).

$$\frac{X}{Q} = \frac{1}{3600\pi\sigma_y \cdot \sigma_z \cdot u} \exp\left(- \frac{H^2}{2\sigma_z^2} \right) \exp\left(- \frac{\lambda x}{u} \right) \qquad (15)$$

where λ is the decay constant of the radionuclide while the others are the same as difined in Section 3. The effective height H of the source is chosen to be 50m for this exercise.

The relative concentration is calculated for every direction using the hourly meteorological data and the effective release time. If there is no lack in data, the total number in a year is 8760. The calculated values of

speeds of the propeller data (because the mean wind speed is now assumed to be 0.1 m/s), those supersonic wind speeds with values 0.5 m/s $\leq$ u $\leq$ 1 m/s will yield a smaller sum of the inverse of wind speeds compared to the corresponding wind speeds of the propeller data (because our earlier correlation study shows that all wind speeds $\leq$ 1 m/s obtained by propeller anemometer are approximately 0.5 m/s less than those obtained by supersonic anemometer). As the total number of calm at 10m height of the propeller data is very much larger than that of the supersonic data (column 8 and 9 of Table 2.9), it is clear that the majority of the wind speeds with value less than 0.5 m/s recorded by the propeller anemometer are actually greater than 0.5 m/s. Thus the latter contribution (i.e. wind speeds with 0.5 m/s $\leq$ u $\leq$ 1 m/s) to the sum of the inverse of wind speed has a greater effect in the estimated average air concentrations. This explains why in spite of the fact that the calm condition has been modified to u < 0.1 m/s for the supersonic wind data, the average air concentrations obtained from the supersonic wind data are still much lower compared to those obtained from the propeller wind data.

4. Analysis of atmospheric diffusion at the postulated accident using the propeller and supersonic wind data

In this section we investigate the effect of the propeller and supersonic wind data on the analysis of atmospheric diffusion at the postulated accident.

The air concentration of radionuclides released for the dose calculation at postulated accident is calculated using downwind concentration per unit release multiplied by the total release during the accident. We consider here only the short time release (1 hour effective release time), where by the relative air concentration χ/Q in h/m^3 is given equation (15).

$$\frac{X}{Q} = \frac{1}{3600\pi\sigma_y \cdot \sigma_z \cdot u} \exp\left(- \frac{H^2}{2\sigma_z^2} \right) \exp\left(- \frac{\lambda x}{u} \right) \qquad (15)$$

where λ is the decay constant of the radionuclide while the others are the same as difined in Section 3. The effective height H of the source is chosen to be 50m for this exercise.

The relative concentration is calculated for every direction using the hourly meteorological data and the effective release time. If there is no lack in data, the total number in a year is 8760. The calculated values of

χ/Q including zero values, are arranged in the order from the smallest to the largest. χ/Q value that corresponds to 97 percentile of the annual accumulative frequency for every direction is picked[1]. The maximum of these picked values is used for the radiation dose calculation.

4.1 χ/Q and D/Q values

Table 4.1 shows the χ/Q values at the 97 percentile of the annual accumulative frequency for all the 16 downwind directions. The distances for each direction where the calculations were made are as given in Table 4.1. These are the distances of the supervised area of JAERI Tokai site (with the exception of downwind directions SSW, SW, NW and S which lie outside the supervised area) from NUCEF (Nuclear Fuel Cycle Safety Engineering Research Facility) that yield the maximum χ/Q for each of the direction. The source term of NUCEF is used in this example exercise. For the propeller wind data, the maximum 97 percential value of χ/Q is 2.568 E-9 h/m^3 at wind speed of 2.4 m/s and atmospheric stability type B and it occurs in downwind direction SW at a distance of 0.65km. For the supersonic wind data, the maximum occur at direction WSW for both $u < 0.5$ m/s and $u < 0.1$ m/s calm conditions. Their respective values are 2.351E-9 h/m^3 and 2.312E-9 h/m^3. These two values from the supersonic wind data are approximately the same and they are both lower compared to the corresponding value of the propeller wind data. These results are as expected because of the higher wind speed and the different wind directions measured by the supersonic anemometer. However, the difference between the supersonic and propeller wind data do not show up significantly in the postulated accident calculation owing to the inert method of choosing the maximum 97 percentils value of χ/Q as recommended by the Japan Atomic Energy Satety Commission in the 'Meteorological Guide For Safety Analysis of Nuclear Reactors'.

Table 4.2 shows the relative γ exposure D/Q values at the 97 percentile of the annual accumulative frequency for all the 16 downwind directions. The distance of each direction where the calculations were made are the distances of the supervised area from NUCEF that will yield maximum D/Q value.

The maximum D/Q for both propeller and supersonic wind data occurs at the same direction, WSW. This is because D/Q calculation is not subjected to the influence of wind direction so easily. Here again the maximum D/Q for propeller data is insignificantly higher than those of the supersonic (same for both $u < 0.5$ m/s and $u < 0.1$ m/s calm conditions), as in the case of maximum χ/Q.

4.2 Adult thyroid exposure dose due to the iodine nuclides

A comparison of the adult thyroid exposure doses due to the postulated accidental releases of iodine nuclides calculated using both sets of wind data is made here. The iodine nuclides considered are ^{131}I, ^{132}I, ^{133}I, ^{134}I and ^{135}I. Table 4.3 shows the 97 percentile values of χ/Q for the 16 directions calculated using propeller wind data and Table 4.4a and 4.4b show the 97 percentile values of χ/Q for the 16 directions calculated using supersonic wind data with $u < 0.5$ m/s and $u < 0.1$ m/s calm conditions respectively. The distances of the 16 directions where calculations were made are the distances of the supervised area (with the exception of downwind directions SSW, SW, NW and S) from NUCEF that will give maximum χ/Q for each of the direction. Table 4.5 gives the amount of rare gases and iodine radionuclides released for the postulated accident. The source term of the I, Xe and Kr nuclides in Table 4.5 is estimated from the inventory of NUCEF. The dose factors for the iodine radionuclides are from ICRP Publication 30. The values at downwind direction WSW are used to calculate the adult thyroid exposure dose. The adult thyroid exposure doses estimated from these iodine radionuclides considering and not considering the decay of individual iodine nuclide using the propeller wind data are 20.35 mrem and 21.43 mrem respectively (Table 4.6). In the case of supersonic, the estimated doses taking into consideration the decay factor for $u < 0.5$ m/s and $u < 0.1$ m/s calm conditions are 19.01 mrem and 18.99 mrem respectively. Their respective doses without considering the decay of the individual radionuclide are 20.17 mrem and 19.84 mrem. The estimated doses without considering the decay of individual iodine nuclides are only slightly higher ($\simeq$ 5%) than those with individual nuclide decay taken into consideration. Thus the decay factor of the individual iodine nuclides has little effect on the estimated adult thyroid exposure dose of the postulated accident. The dose estimated without considering the decay of individual iodine nuclides being more conservative and convenient to calculate is thus a valid and useful indication of the adult thyroid exposure dose due to the postulated releases of iodine. The doses estimated using the propeller wind data are also higher than those using the supersonic wind data. Although the difference is not large and is only about 6%, the doses estimated using the supersonic wind data are more accurate and realistic because of the accurate low wind speeds and wind directions used in the calculations. The inert method of choosing the maximum 97 percentile value of χ/Q is partly the reason why the difference in

the doses estimated using the 2 different wind data being small. The modification of the assumed wind speed of the calm condition from $_{c}U$ = 0.5 m/s to $_{c}U$ = 0.1 m/s has resulted almost no difference in the doses estimated. This analysis thus shows that estimation of the adult thyroid exposure dose for the postulated accident basing on the contributions of individual iodine nuclides without considering their decay factors and using the supersonic wind data without modifying the assumed wind speed of the calm for atmospheric dispersion is sufficiently accurate and valid.

4.3 External γ whole body exposures due to the Xe and Kr nuclides

The external γ whole body exposures due to the release of Xe and Kr radionuclides in a postulated accident are calculated using the two sets of wind data and considering the decay of each radionuclide. The Xe nuclides considered are ^{131m}Xe, ^{133m}Xe, ^{133}Xe, ^{135}Xe, ^{137}Xe, ^{138}Xe and ^{139}Xe while the Kr nuclides considered are ^{85m}Kr, ^{85}Kr, ^{87}Kr, ^{88}Kr, ^{89}Kr and ^{90}Kr. The amount that these nuclides are released in a postulated accident are as given in Table 4.5.

The 97 percentile values of D/Q for the 16 downwind directions calculated using the propeller and supersonic wind data are given in Tables 4.7a and 4.7b for Xe nuclides and Tables 4.8a and 4.8b for Kr nuclides respectively. In the case of the supersonic wind data, only the 97 percentile values for u < 0.5 m/s calm condition is shown. This is because very little difference is observed for the corresponding values obtained for u < 0.1 m/s calm condition. The distances of the 16 downwind directions where D/Q calculations are made are the distances of the supervised area from NUCEF that will give maximum D/Q for each of the direction. The D/Q values at downwind direction WSW are used to calculate the external γ whole body exposures. The values obtained for the Xe and Kr nuclides using the supersonic wind data are 6.01 mrem and 5.74 mrem respectively (Table 4.9). Their corresponding values calculated using the propeller wind data are 6.81 mrem and 6.36 mrem respectively. Thus the total γ exposure doses due to the release of Xe and Kr nuclides calculated using supersonic and propeller wind data are 11.75 mrem and 13.17 mrem respectively. Here again, the difference between the dose values calculated using the two different wind data sets is not large ($\simeq$ 11%) owing to the inert method of choosing the maximum 97 percentile values. Nonetheless, the values calculated using the propeller wind data are as usual larger than those of the supersonic wind

data. Thus, the external γ whole body exposure calculated using propeller wind data is more conservative, however the exposure value obtained using the supersonic wind data is more accurate and realistic owing to the accurate low wind speeds and wind directions measured by the supersonic anemometer and used in the atmospheric dispersion analysis.

From the maximum D/Q values obtained (also in WSW direction) for rare gases (not including iodine nuclides) in Table 4.2 and using a γ radiation release of 1.12×10^4 MeV.Ci, we calculated the external γ whole body exposure due to the rare gases without considering the decay of each radionuclides. The exposures calculated using the supersonic and propeller wind data are 23.51 mrem and 25.86 mrem respectively. Again, the propeller wind data gives more conservative exposure although this value is not as accurate as that of the supersonic wind data. Both the exposures due to the release of rare gases are higher by a factor of two with respect to the exposures calculated basing on individual Xe and Kr nuclides with their decay taken into consideration. This is because in the case of the rare gases calculation, no decay factor is taken into account. Thus for a more accurate and realistic estimation of the external γ whole body exposure for the postulated accident, the estimation should base on the contributions of individual radionuclides with their decay factors considered and use the supersonic wind data for atmospheric dispersion analysis. However, for fast, convenient and conservative external γ whole body exposure estimation of the postulated accident, calculation based on the releases of rare gases with no decay considered is a better choice.

5. Conclusions

The statistical analyses and comparisons of the wind data obtained by the propeller and supersonic anemometers for the year of 1987 in Japan Atomic Energy Research Institute, Tokai Establishment show relatively large difference occurs in the wind speeds and direction measurements when the wind speed is less than 1 m/s. For wind speeds less than 1 m/s, the propeller readings are generally about 0.5 m/s less than those of the supersonic readings. The number of calm recorded thus differ, with the supersonic wind data having much less calm. These differences affect the annual percentage frequency distribution of stability category, the sum of the inverse of wind speed and the frequency distribution of wind direction that are used in

data. Thus, the external γ whole body exposure calculated using propeller wind data is more conservative, however the exposure value obtained using the supersonic wind data is more accurate and realistic owing to the accurate low wind speeds and wind directions measured by the supersonic anemometer and used in the atmospheric dispersion analysis.

From the maximum D/Q values obtained (also in WSW direction) for rare gases (not including iodine nuclides) in Table 4.2 and using a γ radiation release of 1.12×10^4 MeV.Ci, we calculated the external γ whole body exposure due to the rare gases without considering the decay of each radionuclides. The exposures calculated using the supersonic and propeller wind data are 23.51 mrem and 25.86 mrem respectively. Again, the propeller wind data gives more conservative exposure although this value is not as accurate as that of the supersonic wind data. Both the exposures due to the release of rare gases are higher by a factor of two with respect to the exposures calculated basing on individual Xe and Kr nuclides with their decay taken into consideration. This is because in the case of the rare gases calculation, no decay factor is taken into account. Thus for a more accurate and realistic estimation of the external γ whole body exposure for the postulated accident, the estimation should base on the contributions of individual radionuclides with their decay factors considered and use the supersonic wind data for atmospheric dispersion analysis. However, for fast, convenient and conservative external γ whole body exposure estimation of the postulated accident, calculation based on the releases of rare gases with no decay considered is a better choice.

5. Conclusions

The statistical analyses and comparisons of the wind data obtained by the propeller and supersonic anemometers for the year of 1987 in Japan Atomic Energy Research Institute, Tokai Establishment show relatively large difference occurs in the wind speeds and direction measurements when the wind speed is less than 1 m/s. For wind speeds less than 1 m/s, the propeller readings are generally about 0.5 m/s less than those of the supersonic readings. The number of calm recorded thus differ, with the supersonic wind data having much less calm. These differences affect the annual percentage frequency distribution of stability category, the sum of the inverse of wind speed and the frequency distribution of wind direction that are used in

calculating the average air concentration and γ exposure rate due to the radioactive releases for normal operation of nuclear power plant.

The average air concentrations and γ exposure rates for most of the directions calculated using the supersonic wind data at 40m height are generally lower than those calculated using the propeller wind data. The overall shapes of the curves plotted using the two different wind data are similar if the number of calm is low. Both the average air concentrations and the ground level external γ exposure rates due to the radioactive cloud are overestimated when calculated using the propeller wind data. When the 10m wind data obtained from the two different anemometer are used to calculated the average air concentrations, the decrease in all the directions of the supersonic case is more prominent. The maximum decrease at S downwind direction is as high as 72%. This is due to the greater number of low wind speeds that occurs at lower altitude and thus the larger influence of calm from the propeller wind data. The influence of the larger number of calm is also indicated by the slight shift between the two average air concentration curves plotted. As supersonic anemometer can measure wind speed to as low as 0.01 m/s, more realistic and accurate estimation of the average air concentrations and exposure rates using supersonic wind data can be resulted. The analysis also shows that if the number of calm is low, the definition of the calm condition as given by the Japan Atomic Energy Satety Commission for the statistical analysis of atmospheric dispersion requires no modification. However if the number of occurrence of calm is large, a more accurate and realistic estimation of the average air concentration and ground level external γ exposure rates due to the normal operation of nuclear power plant can be obtained only if the actual low wind speeds and wind directions are used in the statistical analysis of the atmospheric dispersion.

When the two different sets of propeller and supersonic wind data are used in the atmospheric diffusion analysis of postulated accident, the estimated adult thyroid exposure doses due to the iodine nuclides do not differ significantly. The dose obtained using the propeller wind data is again slightly larger (about 6%) and more conservative. The decay of the individual iodine nuclides has little effect on the estimated doses. Changing the assumed mean wind speed of the calm condition to 0.1 m/s also has resulted almost no difference in the doses estimated. The inert method of choosing the maximum 97 percentile value of χ/Q is partly the reason for the small difference in all the doses estimated. The results show that the

adult thyroid exposure dose of the postulated accident is sufficiently accurate and valid when estimated basing on the contributions of individual iodine nuclides without considering their decay and using the supersonic wind data without having to modify the assumed mean wind speed of the calm.

Similarly, when the external γ whole body exposures due to the Xe and Kr nuclides are estimated using the two different sets of wind data, the exposure obtained using the propeller wind data is also larger ($\sim$ 11%) and more conservative than that of the supersonic wind data. The 97 percentile values of D/Q obtained for $u < 0.5$ m/s and $u < 0.1$ m/s calm conditions are almost the same. The estimated external γ whole body exposure due to the rare gases (not including iodine nuclides) is higher by a factor of two when compared to the exposure calculated basing on individual Xe and Kr nuclides with their decay considered. Thus the analysis shows that a more accurate and realistic estimation of the external γ whole body exposure for the postulated accident should base on the contributions of individual radionuclides with their decay considered and use the supersonic wind data for atmospheric dispersion analysis. However for fast, convenient and conservative estimation, calculation based on the releases of rare gases with no decay considered is a better choice.

The performance and routine usage of the supersonic anemometer in Japan Atomic Energy Research Institute, Tokai Establishment for more than a year has shown that the supersonic anemometer, under all conditions is highly reliable, stable and capable of yielding accurate wind speed data especially under low wind speed condition. Thus, supersonic instead of propeller wind data are to be used in the statistical analysis of atmospheric dispersion and dose estimation since supersonic anemometer can give accurate wind speed to as low as 0.01 m/s.

Acknowledgements

We would like to thank the Japan Science and Technology Agency for the Scientist Exchange Program fellowship awarded to one of the authors, S. J. Hu for his stay in the Department of Health Physics, Japan Atomic Energy Research Institute during which this work was performed. we wishes to thank Dr. J. Akaishi, Manager of the Radiation Control Division 1 for the facilities and help rendered us in completing this project. We also wishes to thank Mr. M. Taki of Radiation Control Division 1 for our help in the computing.

adult thyroid exposure dose of the postulated accident is sufficiently accurate and valid when estimated basing on the contributions of individual iodine nuclides without considering their decay and using the supersonic wind data without having to modify the assumed mean wind speed of the calm.

Similarly, when the external γ whole body exposures due to the Xe and Kr nuclides are estimated using the two different sets of wind data, the exposure obtained using the propeller wind data is also larger ($\sim$ 11%) and more conservative than that of the supersonic wind data. The 97 percentile values of D/Q obtained for $u < 0.5$ m/s and $u < 0.1$ m/s calm conditions are almost the same. The estimated external γ whole body exposure due to the rare gases (not including iodine nuclides) is higher by a factor of two when compared to the exposure calculated basing on individual Xe and Kr nuclides with their decay considered. Thus the analysis shows that a more accurate and realistic estimation of the external γ whole body exposure for the postulated accident should base on the contributions of individual radionuclides with their decay considered and use the supersonic wind data for atmospheric dispersion analysis. However for fast, convenient and conservative estimation, calculation based on the releases of rare gases with no decay considered is a better choice.

The performance and routine usage of the supersonic anemometer in Japan Atomic Energy Research Institute, Tokai Establishment for more than a year has shown that the supersonic anemometer, under all conditions is highly reliable, stable and capable of yielding accurate wind speed data especially under low wind speed condition. Thus, supersonic instead of propeller wind data are to be used in the statistical analysis of atmospheric dispersion and dose estimation since supersonic anemometer can give accurate wind speed to as low as 0.01 m/s.

Acknowledgements

We would like to thank the Japan Science and Technology Agency for the Scientist Exchange Program fellowship awarded to one of the authors, S. J. Hu for his stay in the Department of Health Physics, Japan Atomic Energy Research Institute during which this work was performed. we wishes to thank Dr. J. Akaishi, Manager of the Radiation Control Division 1 for the facilities and help rendered us in completing this project. We also wishes to thank Mr. M. Taki of Radiation Control Division 1 for our help in the computing.

References

(1) Japan Atomic Energy Safety Commission "Meteorological guide for safety analysis of nuclear power reactors" (1977).

(2) Maede, P. J., "The effects of meteorological factors on the dispersion of airborne material", Ressegna Int. Electtronica e Nucleare e Rassegna Rome 1959, Vol. 11, 107-130 (1959).

(3) ICRP Publication 30. "Limits for intakes of radionuclides by workers" (1979).

(4) K. Imai and T. Iijima, "Assessment of γ-exposure due to a radioactive cloud released from a point source", Health Phys. 17, 207 (1970).

(5) G. E. Chabot, Jr., K. W. Skrable and H. L. Wedlick, Health Phys. 21, 471 (1971).

Table 1.1 The instruments and characteristics for the ordinary observation

Items	Instruments	Units	The Smallest No. of Units	The Height
Wind direction	(1) Anemometer (2) Anemometer for light wind	16 directions (22.5° each)	1	(1) About 10 m above ground for the representative wind for the site
Wind speed	(1) Anemometer (2) Anemometer for light wind	m/s	0.1	(2) At the representative chimney height
Insolation	Pyrheliometer	cal/cm^2.h	0.5	About 1.5 m above ground as a rule
Net radiation	Net radiometer	cal/cm^2.h	0.1	About 1.5 m above ground
Temperature gradient	Thermometer	°C	0.1	(1) About 10 m above ground (2) About the chimney height (3) The various heights in the lower atmosphere

Table 1.2 Definitions and units of statistical item

Item	Definitions	Units
Calm	Wind Speed < 0.5 m/s	–
Air Temperature	1.5 m above the ground	°C
Temperature Lapse Rate	$\frac{\text{Air Temp. (40 m) − Air Temp. (1.5 m)}}{38.5} \times 100$	°C/100 m
Stability	See Table 1.3	–
Solar Radiation	Jan.~ Mar., Sept.~Dec.--- 8~16 o'clock Apr., May, July, Aug.--- 7~17 o'clock June ---------- 7~18 o'clock	kw/m²
Net Radiation	Jan.~ Mar., Sept.~Dec.--- 17~7 o'clock Apr., May, July, Aug.--- 18~6 o'clock June ---------- 19~6 o'clock	kw/m²

Table 1.3 Classification of stability

Wind Speed (u)	Solar Radiation (S) kw/m²				Net Radiation (N) kw/m²		
m/s	$S \geq 0.60$	$0.60 > S \geq 0.30$	$0.30 > S \geq 0.15$	$0.15 > S$	$N \geq -0.020$	$-0.020 > N \geq -0.040$	$-0.040 > N$
$u < 2$	A	A–B	B	D_1	D_2	G	G
$2 < u < 3$	A–B	B	C	D_1	D_2	E	F
$3 < u < 4$	B	B–C	C	D_1	D_2	D_2	E
$4 < u < 6$	C	C–D	D_1	D_1	D_2	D_2	D_2
$6 < u$	C	D_1	D_1	D_1	D_2	D_2	D_2

Table 2.1a Monthly and yearly averages of the meteorological data (supersonic)

		MONTH	1	2	3	4	5	6	7	8	9	10	11	12	AVERAGE
	10MI	%	2.2	2.1	2.0	1.5	5.1	3.5	3.2	3.1	1.4	3.3	1.8	1.9	2.6
CALM	20MI	%	0.1	0.1	0.5	0.0	1.5	1.4	2.4	1.5	0.3	0.7	0.4	0.3	0.8
	40MI	%	0.1	0.1	0.5	0.3	1.3	0.6	0.9	0.9	0.4	0.7	0.4	0.3	0.6
	10MI	M/S	1.8	2.0	2.2	2.3	2.1	2.3	1.7	2.1	2.7	2.2	2.0	2.0	2.1
WIND SPEED	20MI	M/S	2.8	3.0	3.1	3.2	2.8	3.0	2.3	2.8	3.6	3.1	3.0	2.9	3.0
	40MI	M/S	4.0	4.3	4.2	4.3	4.0	4.2	3.3	3.9	4.9	4.3	4.2	4.1	4.1
AIR TEMPERATURE	1.5MI	C	2.9	4.2	6.9	11.0	15.7	18.1	23.0	23.8	20.9	16.4	9.9	5.2	13.2
HUMIDITY	1.5MI	%	58.2	60.2	63.7	67.7	73.9	78.4	80.7	81.3	78.8	76.0	69.4	69.0	71.4
SOLAR RADIATION	5 MIMJ/SQ(M).DAY		8.4	9.8	11.8	16.2	16.0	16.1	15.6	17.0	11.3	9.8	7.7	6.9	12.2
NET RADIATION	1.5MIMJ/SQ(M).DAY		2.3	2.2	1.8	1.5	1.4	1.1	0.8	0.9	1.2	1.6	1.9	2.0	1.6
PRECIPITATION		MM	39.5	52.0	90.5	44.0	109.0	98.5	100.5	95.0	162.5	144.5	54.0	40.5	1030.5

Table 2.1b Monthly and yearly averages of the meteorological data (propeller)

		MONTH	1	2	3	4	5	6	7	8	9	10	11	12	AVERAGE
	10MI	%	13.2	13.3	11.4	13.5	23.5	15.7	19.1	16.8	10.2	16.1	13.6	13.1	15.0
CALM	20MI	%	3.0	2.6	2.8	2.8	6.7	4.4	7.3	5.0	2.9	4.3	2.8	3.1	4.0
	40MI	%	0.9	1.5	1.2	1.4	3.4	2.6	5.1	3.6	1.4	1.7	1.0	2.0	2.2
	10MI	M/S	1.3	1.6	1.8	2.0	1.8	2.0	1.5	1.9	2.6	1.9	1.6	1.4	1.8
WIND SPEED	20MI	M/S	2.1	2.5	2.6	2.9	2.7	2.9	2.2	2.7	3.6	2.8	2.5	2.3	2.7
	40MI	M/S	3.3	3.7	3.7	3.9	3.6	3.9	3.0	3.5	4.7	3.9	3.6	3.5	3.7
AIR TEMPERATURE	1.5MI	C	2.9	4.2	6.9	11.0	15.7	18.1	23.0	23.8	20.9	16.4	9.9	5.2	13.2
HUMIDITY	1.5MI	%	58.2	60.2	63.7	67.7	73.9	78.4	80.7	81.3	78.8	76.0	69.4	69.0	71.4
SOLAR RADIATION	5 MIMJ/SQ(M).DAY		8.4	9.8	11.8	16.2	16.0	16.1	15.6	17.0	11.3	9.8	7.7	6.9	12.2
NET RADIATION	1.5MIMJ/SQ(M).DAY		2.3	2.2	1.8	1.5	1.4	1.1	0.8	0.9	1.2	1.6	1.9	2.0	1.6
PRECIPITATION		MM	39.5	52.0	90.5	44.0	109.0	98.5	100.5	95.0	162.5	144.5	54.0	40.5	1030.5

Table 2.2a Annual percentage frequency distribution of wind direction (supersonic)

I W.D.I	CALM	NNE	NE	ENE	E	ESE	SE	SSE	S	SSW	SW	WSW	W	WNW	NW	NNW	NI
I 10MHI	2.6	7.7	12.3	7.7	4.5	3.0	3.4	3.5	4.5	3.9	3.8	3.2	6.1	17.8	10.6	4.2	1.41
I 20MHI	0.8	13.8	11.1	2.6	1.4	1.6	2.8	3.4	5.4	3.2	4.9	4.5	6.0	11.4	18.0	7.0	2.21
I 40MHI	0.6	8.6	14.2	7.4	4.0	2.9	3.1	5.1	3.1	3.7	4.4	3.8	4.3	9.9	16.3	6.7	2.11

Table 2.2b Annual percentage frequency distribution of wind direction (propeller)

I W.D.I	CALM	NNE	NE	ENE	E	ESE	SE	SSE	S	SSW	SW	WSW	W	WNW	NW	NNW	NI
I 10MHI	15.0	10.8	10.1	5.7	3.8	2.6	2.9	3.0	2.9	2.5	2.6	2.3	3.7	7.1	14.5	5.7	4.81
I 20MHI	4.0	6.9	14.0	7.8	4.1	2.9	2.5	3.2	4.4	2.4	4.3	3.6	4.6	8.2	17.3	6.4	3.41
I 40MHI	2.2	9.0	13.8	6.6	3.2	2.7	2.8	4.8	3.1	3.2	4.4	3.8	4.1	9.1	16.5	6.8	4.01

Table 2.3a Annual percentage frequency distribution of stability category

Stability	A	A-B	B	B-C	C	C-D	D1	D2	E	F	G
Frequency (Propeller)	2.1	10.5	9.5	1.7	3.6	1.4	12.6	25.6	2.0	2.0	29.0
Frequency (Supersonic)	1.5	8.7	10.3	2.1	4.4	1.7	12.7	26.0	3.5	4.3	24.8

Table 2.3b Annual percentage frequency distribution of stability category

Stability	A	B	C	D	E	F
Frequency (Propeller)	2.1	20	5.3	39.6	2	31
Frequency (Supersonic)	1.5	19	6.5	40.4	3.5	29.1

Table 2.4a Sum of 1/(W.SPD) for wind direction and stability (40m height, propeller)

STATISTICS FROM JAN. TO DEC.

	NNE	NE	ENE	E	ESE	SE	SSE	S	SSW	SW	WSW	W	WNW	NW	NNW	N	TOTL
A	0.07	3.94	11.95	17.72	8.63	8.26	8.15	2.10	3.86	4.12	7.28	4.23	5.14	5.43	2.25	0.68	93.81
B	14.99	40.35	69.09	63.83	63.79	68.64	73.03	17.89	22.42	34.05	50.79	49.93	72.89	96.90	60.66	28.93	828.17
C	5.76	26.83	11.76	2.03	1.58	1.33	11.70	3.77	3.59	6.27	1.08	0.58	2.48	6.47	1.78	0.70	87.72
D	131.13	194.06	92.90	44.36	32.67	26.09	45.52	57.48	47.02	50.09	47.54	57.27	105.79	197.47	108.81	84.16	1322.36
E	9.13	9.47	4.56	0.0	0.22	0.0	0.33	2.07	1.31	1.20	0.35	0.28	0.90	4.15	0.50	0.85	35.32
F	53.82	55.54	33.56	30.17	21.55	22.81	26.05	35.55	48.01	47.46	68.51	74.69	191.66	298.23	128.35	79.20	1215.17
TOTL	214.90	330.19	223.82	158.11	128.43	127.14	164.79	118.86	126.21	143.20	175.56	186.98	378.85	608.66	302.35	194.52	

Table 2.4b Mean 1/(W.SPD) for wind direction and stability (40m height, propeller)

STATISTICS FROM JAN. TO DEC.

	NNE	NE	ENE	E	ESE	SE	SSE	S	SSW	SW	WSW	W	WNW	NW	NNW	N	TOTL
A	2.00	0.76	0.56	0.53	0.65	0.50	0.40	0.51	0.63	0.40	0.42	0.51	0.55	0.48	0.54	0.62	0.51
B	0.64	0.51	0.37	0.50	0.45	0.44	0.35	0.53	0.45	0.41	0.51	0.50	0.53	0.54	0.60	0.72	0.47
C	0.21	0.19	0.22	0.25	0.31	0.26	0.21	0.22	0.14	0.14	0.15	0.14	0.19	0.16	0.17	0.23	0.19
D	0.23	0.23	0.39	0.55	0.60	0.56	0.45	0.41	0.41	0.32	0.60	0.61	0.54	0.47	0.56	0.53	0.38
E	0.21	0.22	0.20	0.0	0.22	0.0	0.32	0.23	0.18	0.17	0.17	0.14	0.22	0.16	0.16	0.21	0.20
F	0.42	0.46	0.47	0.65	0.78	0.70	0.62	0.49	0.54	0.48	0.51	0.46	0.43	0.37	0.44	0.50	0.45
TOTL	0.27	0.27	0.38	0.53	0.53	0.50	0.38	0.43	0.43	0.36	0.51	0.50	0.47	0.41	0.50	0.54	

Table 2.5a Sum of 1/(W.SPD) for wind direction snd stability (40m height, supersonic u < 0.5 m/s)

STATISTICS FROM JAN. TO DEC.

	NNE	NE	ENE	E	ESE	SE	SSE	S	SSW	SW	WSW	W	WNW	NW	NNW	N	TOTL
A	1.27	1.89	6.78	16.01	3.45	4.90	1.88	2.74	3.86	4.33	7.39	3.21	3.17	2.66	1.59	0.61	65.73
B	14.57	23.31	63.32	59.93	59.84	58.58	62.28	9.64	28.43	38.87	42.23	43.29	54.03	53.96	45.49	14.03	671.79
C	6.00	27.04	14.78	5.66	2.23	3.93	16.79	2.93	4.63	3.57	0.70	1.52	7.12	10.96	3.02	0.40	111.29
D	119.74	176.06	88.01	45.14	22.38	25.96	46.05	44.48	41.21	40.80	41.16	47.49	83.91	143.17	85.26	31.60	1082.41
E	9.58	10.53	5.34	0.44	0.20	0.27	0.29	2.73	0.87	1.12	0.0	0.51	5.81	17.59	3.58	0.48	59.32
F	43.66	42.47	32.38	29.94	19.76	15.42	23.54	30.99	36.64	50.51	58.31	67.47	138.39	191.47	91.22	34.72	906.88
TOTL	194.82	281.31	210.61	157.13	107.85	109.06	150.82	93.51	115.63	139.19	149.79	163.49	292.43	419.81	230.15	81.84	

Table 2.5b Mean 1/(w.spd) for wind direction and stability (40m height, supersonic u < 0.5 m/s)

STATISTICS FROM JAN. TO DEC.

	NNE	NE	ENE	E	ESE	SE	SSE	S	SSW	SW	WSW	W	WNW	NW	NNW	N	TOTL
A	1.15	0.60	0.46	0.55	0.47	0.67	0.44	0.65	0.46	0.37	0.50	0.43	0.43	0.50	0.49	0.56	0.50
B	0.62	0.36	0.34	0.41	0.38	0.36	0.33	0.48	0.40	0.38	0.42	0.46	0.42	0.44	0.49	0.57	0.40
C	0.21	0.19	0.20	0.26	0.27	0.25	0.21	0.20	0.13	0.13	0.13	0.18	0.20	0.19	0.17	0.19	0.19
D	0.23	0.20	0.31	0.46	0.46	0.48	0.34	0.33	0.34	0.31	0.52	0.52	0.39	0.30	0.44	0.45	0.31
E	0.20	0.21	0.20	0.21	0.19	0.26	0.28	0.22	0.17	0.15	0.0	0.12	0.19	0.19	0.17	0.15	0.19
F	0.36	0.36	0.44	0.57	0.58	0.50	0.50	0.39	0.43	0.44	0.44	0.38	0.31	0.29	0.35	0.44	0.36
TOTL	0.26	0.22	0.32	0.45	0.42	0.40	0.33	0.35	0.35	0.35	0.45	0.43	0.34	0.29	0.39	0.45	

Table 2.6a Sum of 1/(W.SPD) for wind direction and stability (10m height, propeller)

STATISTICS FROM JAN. TO DEC.

	NNE	NE	ENE	E	ESE	SE	SSE	S	SSW	SW	WSW	W	WNW	NW	NNW	N	TOTL
A	7.42	16.98	6.16	19.22	8.85	10.06	9.15	8.17	5.63	5.29	12.64	7.24	8.54	5.40	4.17	4.62	139.54
B	67.99	93.83	95.69	98.68	84.39	82.58	77.78	49.09	39.83	57.34	54.13	102.16	104.67	214.83	96.93	55.29	1375.20
C	18.08	29.44	19.21	4.44	3.34	2.69	9.03	12.76	7.17	6.85	2.85	1.84	3.09	14.30	8.82	6.33	150.25
D	338.53	263.27	203.72	118.28	70.29	84.59	87.29	75.93	83.45	78.14	76.37	137.45	283.54	589.06	232.23	166.59	2888.71
E	20.68	13.11	3.93	1.28	0.46	0.0	1.53	1.80	2.13	1.70	0.93	1.00	1.67	11.17	3.74	4.05	69.19
F	201.38	164.07	123.56	88.99	70.03	76.88	72.98	72.25	85.35	118.72	165.57	285.24	583.36	918.44	277.94	184.98	3489.75
TOTL	654.08	580.70	452.27	330.88	237.37	256.80	257.76	220.00	223.57	268.05	312.48	534.93	984.87	1753.19	623.82	421.85	

Table 2.6b Mean 1/(W.SPD) for wind direction and stability (10m height, propeller)

STATISTICS FROM JAN. TO DEC.

	NNE	NE	ENE	E	ESE	SE	SSE	S	SSW	SW	WSW	W	WNW	NW	NNW	N	TOTL
A	0.72	0.69	0.86	0.75	0.72	0.62	0.75	1.00	0.69	1.03	0.88	0.88	0.75	0.73	1.00	0.64	0.76
B	0.71	0.66	0.67	0.66	0.65	0.65	0.62	0.62	0.74	0.83	1.02	1.07	1.05	1.00	0.89	0.87	0.79
C	0.31	0.30	0.36	0.33	0.36	0.38	0.34	0.35	0.29	0.29	0.40	0.36	0.38	0.33	0.35	0.33	0.33
D	0.52	0.48	0.75	0.86	1.00	0.92	0.94	0.73	0.85	0.91	1.36	1.42	1.38	1.17	1.01	0.71	0.83
E	0.38	0.40	0.38	0.42	0.45	0.0	0.50	0.44	0.42	0.42	0.45	0.49	0.41	0.36	0.37	0.40	0.39
F	1.15	1.23	1.33	1.57	1.54	1.55	1.54	1.31	1.29	1.42	1.35	1.40	1.27	1.20	1.31	1.24	1.28
TOTL	0.62	0.60	0.79	0.86	0.89	0.88	0.84	0.76	0.87	0.99	1.22	1.30	1.25	1.12	1.06	0.87	

Table 2.7a Sum of 1/(W.SPD) for wind direction and stability (10m height, supersonic u < 0.5 m/s)

STATISTICS FROM JAN. TO DEC.

	NNE	NE	ENE	E	ESE	SE	SSE	S	SSW	SW	WSW	W	WNW	NW	NNW	N	TOTL
A	0.10	3.36	6.18	14.97	12.16	5.32	2.90	5.56	6.81	6.32	9.10	8.51	5.44	2.93	3.31	0.05	93.03
B	13.79	30.16	65.63	91.70	82.10	89.11	73.14	46.48	52.51	66.88	84.47	79.27	124.83	83.68	46.00	14.631	044.37
C	8.68	36.54	28.92	9.97	3.47	5.19	10.39	21.70	9.94	9.55	1.04	4.90	18.68	12.36	5.50	0.81	187.63
D	200.52	244.02	177.33	95.45	46.85	58.26	87.68	70.59	95.65	85.51	84.32	145.54	333.15	237.01	117.64	44.262	123.77
E	19.87	14.07	14.29	0.49	0.93	0.45	0.0	4.53	2.80	3.13	0.0	1.96	34.96	15.26	5.71	0.91	119.36
F	101.92	51.40	62.70	85.25	31.73	49.20	43.33	53.32	100.05	115.20	166.03	315.49	618.22	304.37	115.54	54.652	268.39
TOTL	344.88	379.55	355.04	297.84	177.23	207.52	217.45	202.18	267.75	286.58	344.96	555.671	135.29	655.61	293.69	115.30	

Table 2.7b Mean 1/(W.SPD) for wind direction snd stability (10m height, supersonic u < 0.5 m/s)

STATISTICS FROM JAN. TO DEC.

	NNE	NE	ENE	E	ESE	SE	SSE	S	SSW	SW	WSW	W	WNW	NW	NNW	N	TOTL
A	2.00	1.07	0.66	0.65	0.69	0.57	0.69	0.76	0.73	0.76	0.79	0.90	0.72	0.68	0.79	2.00	0.72
B	0.79	0.53	0.47	0.57	0.53	0.52	0.50	0.49	0.69	0.75	1.02	0.87	0.67	0.73	0.66	0.77	0.62
C	0.35	0.29	0.33	0.42	0.37	0.38	0.38	0.30	0.30	0.34	0.50	0.39	0.37	0.31	0.33	0.39	0.33
D	0.44	0.30	0.52	0.80	0.85	0.85	0.87	0.44	0.73	0.73	1.34	1.15	0.76	0.65	0.86	0.97	0.60
E	0.39	0.36	0.42	0.48	0.45	0.43	0.0	0.40	0.38	0.43	0.0	0.38	0.40	0.38	0.34	0.44	0.39
F	0.78	0.74	0.84	1.12	1.11	1.16	1.12	0.95	1.04	1.27	1.23	1.00	0.75	0.79	0.87	0.98	0.89
TOTL	0.51	0.35	0.52	0.73	0.66	0.67	0.68	0.50	0.76	0.84	1.17	0.99	0.71	0.69	0.78	0.93	

Table 2.8a Sun of 1/(W.SPD) for wind direction and stability (40m height, supersonic u < 0.1 m/s)

STATISTICS FROM JAN. TO DEC.

	NNE	NE	ENE	E	ESE	SE	SSE	S	SSW	SW	WSW	W	WNW	NW	NNW	N	TOTL
A	1.16	1.80	6.66	15.86	3.36	4.81	1.78	2.66	3.75	4.18	10.70	3.05	3.00	2.46	1.37	0.52	67.12
B	13.61	22.46	62.21	58.60	62.54	63.85	66.63	8.88	30.05	37.57	45.92	41.87	58.56	52.15	43.54	13.27	681.71
C	6.00	27.04	14.78	5.66	2.23	3.93	16.79	2.93	4.63	3.57	0.70	1.52	7.12	10.96	3.02	0.40	111.29
D	117.73	176.87	88.30	50.16	40.72	26.83	44.20	48.10	41.73	38.05	46.63	50.59	85.83	147.18	83.77	30.00	1116.69
E	9.58	10.53	5.34	0.44	0.20	0.27	0.29	2.73	0.87	1.12	0.0	0.51	5.81	17.59	3.58	0.48	59.32
F	42.07	47.14	30.54	35.55	21.05	17.53	25.57	29.73	35.00	62.26	60.98	65.11	135.79	198.90	90.59	36.07	933.85
TOTL	190.15	285.83	207.82	166.28	130.09	117.22	155.26	95.03	116.02	146.75	164.93	162.66	296.09	429.23	225.88	80.75	

Table 2.8b Mean 1/(W.SPD) for wind direction and stability (40m height, supersonic u < 0.1 m/s)

STATISTICS FROM JAN. TO DEC.

	NNE	NE	ENE	E	ESE	SE	SSE	S	SSW	SW	WSW	W	WNW	NW	NNW	N	TOTL
A	1.11	0.57	0.46	0.54	0.46	0.66	0.43	0.64	0.45	0.36	0.68	0.42	0.41	0.47	0.44	0.50	0.51
B	0.59	0.35	0.33	0.40	0.40	0.39	0.35	0.45	0.42	0.37	0.45	0.45	0.45	0.43	0.48	0.55	0.40
C	0.21	0.19	0.20	0.26	0.27.	0.25	0.21	0.20	0.13	0.13	0.13	0.18	0.20	0.19	0.17	0.19	0.19
D	0.23	0.20	0.31	0.51	0.78	0.49	0.33	0.35	0.34	0.29	0.59	0.55	0.40	0.31	0.43	0.43	0.32
E	0.20	0.21	0.20	0.21	0.19	0.26	0.28	0.22	0.17	0.15	0.0	0.12	0.19	0.19	0.17	0.15	0.19
F	0.34	0.39	0.42	0.67	0.61	0.56	0.54	0.37	0.42	0.54	0.46	0.37	0.31	0.30	0.35	0.45	0.37
TOTL	0.26	0.23	0.32	0.48	0.50	0.43	0.34	0.36	0.36	0.37	0.49	0.43	0.34	0.30	0.39	0.45	

Table 2.9 Number of calm at each stability category for the propeller and supersonic (u < 0.5 m/s and u < 0.1 m/s) wind data

Stability	40 m height			20 m height			10 m height		
	Propeller	Supersonic		Propeller	Supersonic		Propeller	Supersonic	
	u<0.5m/s	u<0.5m/s	u<0.1m/s	u<0.5m/s	u<0.5m/s	u<0.1m/s	u<0.5m/s	u<0.5m/s	u<0.1m/s
A	1	1	0	1	0	0	1	1	0
A-B	20	7	1	27	2	0	54	18	0
B	14	3	0	21	1	0	47	10	0
B-C	0	0	0	0	0	0	0	0	0
C	0	0	0	0	0	0	0	0	0
C-D	0	0	0	0	0	0	0	0	0
D	81	19	0	142	28	0	501	78	0
E	0	0	0	0	0	0	0	0	0
F	0	0	0	0	0	0	0	0	0
G	69	15	0	148	31	0	679	118	1
Total	185	45	1	339	62	0	1282	215	1

Table 2.10a Sum of 1/(W.SPD) for wind direction and stability (10m height, supersonic u < 0.1 m/s)

STATISTICS FROM JAN. TO DEC.

	NNE	NE	ENE	E	ESE	SE	SSE	S	SSW	SW	WSW	W	WNW	NW	NNW	N	TOTL
A	0.0	3.29	6.08	14.86	12.10	5.25	2.83	5.51	17.11	6.23	8.98	8.29	4.97	2.65	3.19	0.0	101.34
B	15.48	29.02	66.40	94.84	84.42	91.30	74.38	49.01	58.63	81.68	90.11	80.49	118.87	81.28	46.50	13.791	076.21
C	8.68	36.54	28.92	9.97	3.47	5.19	10.39	21.70	9.94	9.55	1.04	4.90	18.68	12.36	5.50	0.81	187.63
D	222.26	252.10	188.48	89.12	49.70	62.27	96.49	83.88	115.26	103.50	104.47	154.30	322.90	220.52	130.21	48.422	243.88
E	19.87	14.07	14.29	0.49	0.93	0.45	0.0	4.53	2.80	3.13	0.0	1.96	34.96	15.26	5.71	0.91	119.36
F	147.52	75.19	69.90	111.67	66.72	80.74	60.45	63.74	123.84	157.33	168.56	306.99	583.37	301.26	139.15	69.982	526.43
TOTL	413.82	410.22	374.07	320.96	217.33	245.20	244.54	228.37	327.58	361.41	373.16	556.93	1083.75	633.33	330.27	133.91	

Table 2.10b Mean 1/(W.SPD) for wind direction and stability (10m height, supersonic u < 0.1 m/s)

STATISTICS FROM JAN. TO DEC.

	NNE	NE	ENE	E	ESE	SE	SSE	S	SSW	SW	WSW	W	WNW	NW	NNW	N	TOTL
A	0.0	1.06	0.65	0.65	0.69	0.56	0.68	0.76	1.65	0.75	0.79	0.89	0.68	0.64	0.77	0.0	0.79
B	0.88	0.52	0.47	0.59	0.54	0.53	0.50	0.51	0.75	0.89	1.07	0.89	0.65	0.72	0.67	0.74	0.64
C	0.35	0.29	0.33	0.42	0.37	0.38	0.38	0.30	0.30	0.34	0.50	0.39	0.37	0.31	0.33	0.39	0.33
D	0.48	0.31	0.55	0.77	0.90	0.91	0.95	0.51	0.87	0.85	1.55	1.21	0.75	0.62	0.96	1.04	0.64
E	0.39	0.36	0.42	0.48	0.45	0.43	0.0	0.40	0.38	0.43	0.0	0.38	0.40	0.38	0.34	0.44	0.39
F	1.08	1.03	0.95	1.45	2.01	1.77	1.45	1.10	1.22	1.59	1.26	1.00	0.73	0.80	1.05	1.25	0.99
TOTL	0.60	0.37	0.54	0.80	0.79	0.79	0.76	0.56	0.90	1.02	1.25	1.01	0.70	0.68	0.88	1.07	

Table 3.1 The groud level external γ exposure rates $D_{\gamma s}$ (Submersion mrem/y) and the average air concentration $\overline{\chi}$ ($\mu Ci/cm^3$) calculated at 1 km distance for 16 downwind directions

	R(M) Dir.(deg)	1000.0 0.0	1000.0 22.5	1000.0 45.0	1000.0 67.5	1000.0 90.0	1000.0 112.5	1000.0 135.0	1000.0 157.5
Propeller	Submerison	6.251E-01	5.591E-01	7.792E-01	6.939E-01	7.628E-01	1.297E+00	2.245E+00	1.140E+00
(u<0.5 m/s)	Air - Conc	1.840E-10	1.646E-10	2.293E-10	2.042E-10	2.245E-10	3.817E-10	6.607E-10	3.354E-10
Supersonic	Submerison	5.403E-01	6.342E-01	7.100E-01	6.371E-01	7.185E-01	1.270E+00	1.983E+00	1.049E+00
(u<0.5 m/s)	Air - Conc	1.590E-10	1.867E-10	2.089E-10	1.875E-10	2.114E-10	3.738E-10	5.835E-10	3.087E-10
Supersonic	Submerison	5.606E-01	6.476E-01	6.662E-01	6.679E-01	7.343E-01	1.308E-01	1.985E+00	1.031E+00
(u<0.1 m/s)	Air - Conc	1.650E-10	1.906E-10	1.961E-10	1.966E-10	2.161E-10	3.850E-10	5.842E-10	3.034E-10

	R(M) Dir.(deg)	1000.0 180.0	1000.0 202.5	1000.0 225.0	1000.0 247.5	1000.0 270.0	1000.0 292.5	1000.0 315.0	1000.0 337.5
Propeller	Submerison	6.920E-01	1.540E+00	2.619E+00	1.452E+00	8.125E-01	7.351E-01	7.533E-01	1.075E+00
(u<0.5 m/s)	Air - Conc	2.037E-10	4.532E-10	7.707E-10	4.273E-10	2.391E-10	2.163E-10	2.217E-10	3.164E-10
Supersonic	Submerison	3.488E-01	1.441E+00	2.518E+00	1.504E+00	8.847E-01	6.963E-01	7.460E-01	1.103E+00
(u<0.5 m/s)	Air - Conc	1.027E-10	4.242E-10	7.409E-10	4.425E-10	2.604E-10	2.049E-10	2.196E-10	3.245E-10
Supersonic	Submerison	3.334E-01	1.428E+00	2.504E+00	1.503E+00	8.845E-01	7.851E-01	7.786E-01	1.111E+00
(u<0.1 m/s)	Air - Conc	9.811E-11	4.203E-10	7.369E-10	4.423E-10	2.603E-10	2.311E-10	2.291E-10	3.270E-10

Table 3.2 The ground level external γ exposure rate D_γ (plume mrem/y) calculated at 1 km distance for 16 downwind directions

R(M)		1000.0	1000.0	1000.0	1000.0	1000.0	1000.0	1000.0	1000.0
Dir.(deg)		0.0	22.5	45.0	67.5	90.0	112.5	135.0	157.5
Propeller	(u<0.5m/s)	9.616E-01	9.545E-01	1.100E+00	1.208E+00	1.430E+00	2.797E+00	4.317E+00	2.316E+00
Supersonic	(u<0.5m/s)	8.182E-01	8.782E-01	1.033E+00	1.064E+00	1.264E+00	2.280E+00	3.244E+00	1.787E+00
	(u<0.1m/s)	8.354E-01	8.818E-01	1.086E+00	1.129E+00	1.277E+00	2.297E+00	3.309E+00	1.771E+00

R(M)		1000.0	1000.0	1000.0	1000.0	1000.0	1000.0	1000.0	1000.0
Dir.(deg)		180.0	202.5	225.0	247.5	270.0	292.5	315.0	337.5
Propeller	(u<0.5m/s)	1.506E+00	1.938E+00	2.690E+00	1.681E+00	1.057E+00	8.627E-01	8.609E-01	1.104E+00
Supersonic	(u<0.5m/s)	7.744E-01	1.690E+00	2.420E+00	1.636E+00	1.072E+00	7.660E-01	7.806E-01	1.064E+00
	(u<0.1m/s)	7.633E-01	1.663E+00	2.448E+00	1.629E+00	1.141E+00	9.109E-01	8.363E-01	1.086E+00

Table 4.1 Maximum 97 percentile χ/Q (h/m^3) of the annual accumulative frequency for the 16 downwind directions

Downwind Direction	Distance (km)	Propeller (u<0.5 m/s)	Supersonic (u<0.5 m/s)	Supersonic (u<0.1 m/s)
SSW	0.87	2.229E-9	2.185E-9	2.185E-9
SW	0.65	2.568E-9	2.264E-9	2.264E-9
WSW	0.46	2.498E-9	2.351E-9	2.312E-9
W	0.69	3.874E-12	1.681E-9	1.681E-9
WNW	0.78	-	-	-
NW	0.90	-	3.562E-11	4.054E-11
NNW	1.26	8.964E-10	1.072E-9	1.072E-9
N	1.78	4.737E-10	3.280E-10	2.665E-10
NNE	0.80	1.285E-11	1.927E-11	1.835E-11
NE	0.38	6.605E-11	5.627E-11	5.378E-11
ENE	0.28	4.671E-25	4.188E-25	4.338E-25
E	0.25	1.552E-28	1.379E-28	1.379E-28
ESE	0.26	2.079E-12	1.801E-12	1.801E-12
SE	0.32	1.247E-10	4.674E-11	4.674E-11
SSE	0.54	1.420E-9	1.222E-9	1.222E-9
S	3.42	1.371E-9	-	-

Table 4.2 Maximum 97 percentile D/Q (μrem/MeV.Ci) of the annual accumulative frequency for the 16 downwind directions

Downwind Direction	Distance (km)	Propeller (u<0.5 m/s)	Supersonic (u<0.5 m/s)	Supersonic (u<0.1 m/s)
SSW	0.85	1.701	1.654	1.654
SW	0.56	2.306	2.035	2.039
WSW	0.46	2.311	2.101	2.101
W	0.69	1.166	1.442	1.484
WNW	0.78	0.589	0.544	0.785
NW	0.87	0.469	0.711	0.782
NNW	1.26	0.722	0.795	0.795
N	1.78	0.395	0.273	0.222
NNE	0.80	0.749	0.737	0.747
NE	0.38	1.756	1.645	1.692
ENE	0.28	2.289	2.220	2.226
E	0.25	2.963	2.557	2.581
ESE	0.26	3.886	2.965	2.965
SE	0.32	4.311	2.967	2.967
SSE	0.54	2.943	2.503	2.543
S	0.95	1.960	0.134	0.128

Table 4.3 97 percentile χ/Q of the annual accumulative frequency for the 16 downwind directions calculated for iodine nuclides with propeller wind data

(unit: h/m^3)

Downwind Direction	Distance (km)	131 I	132 I	133 I	134 I	135 I	131 I (no λ)
SSW	0.87	2.113E-09	1.967E-09	2.098E-09	1.747E-09	2.062E-09	2.229E-09
SW	0.65	2.439E-09	2.311E-09	2.426E-09	2.116E-09	2.395E-09	2.568E-09
WSW	0.46	2.406E-09	2.316E-09	2.397E-09	2.176E-09	2.375E-09	2.498E-09
W	0.69	3.871E-12	3.657E-12	3.849E-12	3.329E-12	3.797E-12	3.874E-12
WNW	0.78	-	-	-	-	-	-
NW	0.9	-	-	-	-	-	-
NNW	1.26	8.463E-10	7.625E-10	8.375E-10	6.425E-10	8.168E-10	8.964E-10
N	1.78	4.511E-10	3.894E-10	4.445E-10	3.057E-10	4.291E-10	4.737E-10
NNE	0.8	1.283E-11	1.201E-11	1.275E-11	1.078E-11	1.255E-11	1.285E-11
NE	0.38	6.599E-11	6.395E-11	6.578E-11	6.073E-11	6.529E-11	6.605E-11
ENE	0.28	4.670E-25	4.563E-25	4.659E-25	4.393E-25	4.633E-25	4.671E-25
E	0.25	1.551E-28	1.520E-28	1.548E-28	1.469E-28	1.541E-28	1.552E-28
ESE	0.26	2.078E-12	2.034E-12	2.074E-12	1.963E-12	2.063E-12	2.079E-12
SE	0.32	1.246E-10	1.213E-10	1.243E-10	1.162E-10	1.235E-10	1.247E-10
SSE	0.54	1.407E-09	1.346E-09	1.401E-09	1.250E-09	1.386E-09	1.420E-09
S	3.42	1.023E-09	7.711E-10	9.947E-10	4.844E-10	9.294E-10	1.371E-09

Table 4.4a 97 percentile χ/Q of the annual accumulative frequency for the 16 downwind directions calculated for iodine nuclides with supersonic wind data (u < 0.5 m/s) (unit: h/m³)

Downwind Direction	Distance (km)	131 I	132 I	133 I	134 I	135 I	131 I (no λ)
SSW	0.87	2.072E-09	1.928E-09	2.057E-09	1.713E-09	2.022E-09	2.185E-09
SW	0.65	2.194E-09	2.079E-09	2.182E-09	1.903E-09	2.154E-09	2.264E-09
WSW	0.46	2.248E-09	2.164E-09	2.240E-09	2.033E-09	2.219E-09	2.351E-09
W	0.69	1.640E-09	1.549E-09	1.631E-09	1.411E-09	1.609E-09	1.681E-09
WNW	0.78	-	-	-	-	-	-
NW	0.9	3.558E-11	3.303E-11	3.532E-11	2.922E-11	3.469E-11	3.562E-11
NNW	1.26	1.006E-09	9.067E-10	9.959E-10	7.640E-10	9.713E-10	1.072E-09
N	1.78	3.123E-10	2.696E-10	3.078E-10	2.116E-10	2.971E-10	3.280E-10
NNE	0.8	1.925E-11	1.802E-11	1.912E-11	1.616E-11	1.882E-11	1.927E-11
NE	0.38	5.621E-11	5.447E-11	5.604E-11	5.173E-11	5.562E-11	5.627E-11
ENE	0.28	4.187E-25	4.091E-25	4.177E-25	3.938E-25	4.154E-25	4.188E-25
E	0.25	1.379E-28	1.351E-28	1.376E-28	1.306E-28	1.369E-28	1.379E-28
ESE	0.26	1.801E-12	1.763E-12	1.797E-12	1.701E-12	1.788E-12	1.801E-12
SE	0.32	4.673E-11	4.550E-11	4.660E-11	4.357E-11	4.631E-11	4.674E-11
SSE	0.54	1.212E-09	1.159E-09	1.206E-09	1.077E-09	1.193E-09	1.222E-09
S	3.42	-	-	-	-	-	-

Table 4.4b 97 percentile χ/Q of the annual accumulative frequency for the 16 downwind directions calculated for iodine nuclides with supersonic wind data (u < 0.1 m/s) (unit: h/m³)

Downwind Direction	Distance (km)	131 I	132 I	133 I	134 I	135 I	131 I (no λ)
SSW	0.87	2.037E-09	1.895E-09	2.022E-09	1.684E-09	1.987E-09	2.185E-09
SW	0.65	2.194E-09	2.079E-09	2.182E-09	1.903E-09	2.154E-09	2.264E-09
WSW	0.46	2.246E-09	2.162E-09	2.237E-09	2.031E-09	2.217E-09	2.312E-09
W	0.69	1.640E-09	1.549E-09	1.631E-09	1.411E-09	1.609E-09	1.681E-09
WNW	0.78	-	-	-	-	-	-
NW	0.9	4.049E-11	3.758E-11	4.019E-11	3.326E-11	3.947E-11	4.054E-11
NNW	1.26	1.006E-09	9.067E-10	9.959E-10	7.640E-10	9.713E-10	1.072E-09
N	1.78	2.538E-10	2.190E-10	2.501E-10	1.720E-10	2.414E-10	2.665E-10
NNE	0.8	1.833E-11	1.716E-11	1.821E-11	1.539E-11	1.793E-11	1.835E-11
NE	0.38	5.373E-11	5.206E-11	5.356E-11	4.944E-11	5.315E-11	5.378E-11
ENE	0.28	4.337E-25	4.237E-25	4.327E-25	4.079E-25	4.302E-25	4.338E-25
E	0.25	1.379E-28	1.351E-28	1.376E-28	1.306E-28	1.369E-28	1.379E-28
ESE	0.26	1.801E-12	1.763E-12	1.797E-12	1.701E-12	1.788E-12	1.801E-12
SE	0.32	4.673E-11	4.550E-11	4.660E-11	4.357E-11	4.631E-11	4.674E-11
SSE	0.54	1.212E-09	1.159E-09	1.206E-09	1.077E-09	1.193E-09	1.222E-09
S	3.42	-	-	-	-	-	-

Table 4.5 Amount each nuclides released in a postulated accident (in Ci)

^{85m}Kr	5.84×10
^{85}Kr	8.52×10^{-3}
^{87}Kr	3.64×10^{2}
^{88}Kr	2.50×10^{2}
^{89}Kr	2.64×10^{3}
^{90}Kr	1.39×10^{2}
^{131m}Xe	5.79×10^{-2}
^{133m}Xe	7.76×10^{-1}
^{133}Xe	1.47×10
^{135m}Xe	4.82×10^{2}
^{135}Xe	1.49×10^{2}
^{137}Xe	3.65×10^{3}
^{138}Xe	3.00×10^{3}
^{139}Xe	3.04×10^{2}
^{131}I	1.22×10^{0}
^{132}I	8.90×10^{1}
^{133}I	1.68×10^{1}
^{134}I	3.74×10^{2}
^{135}I	4.90×10^{1}
γ radiation (except iodine nuclides)	1.12×10^{4} (MeV.Ci)
β radiation	1.38×10^{4} (MeV.Ci)

Table 4.6 The adult thyroid exposure doses due to the release of iodine nuclides with and without decay considered in a postulated accident calculated using propeller and supersonic wind data

(unit : mrem)

Iodine Nuclides Released	Propeller u<0.5 m/s	Supersonic u<0.5 m/s	Supersonic u<0.1 m/s
With decay	20.35	19.01	18.99
Without decay	21.43	20.17	19.84

Table 4.7a 97 percentile D/Q of the annual accumulative frequency for the 16 downwind directions calculated for Xe nuclides with propeller wind data

(unit: μrem/MeV.Ci)

Downwind Direction	Distance (km)	131m Xe	133m Xe	133 Xe	135m Xe	135 Xe	137 Xe	138 Xe	139 Xe
SSW	0.85	6.259E-02	1.086E-01	1.121E-01	3.840E-01	4.566E-01	2.480E-02	9.104E-01	4.423E-04
SW	0.56	8.291E-02	1.498E-01	1.544E-01	6.482E-01	6.220E-01	8.044E-02	1.563E+00	3.799E-03
WSW	0.46	8.963E-02	1.440E-01	1.483E-01	7.046E-01	6.136E-01	1.135E-01	1.723E+00	8.944E-03
W	0.69	3.772E-02	6.212E-02	6.395E-02	2.997E-01	3.050E-01	2.961E-02	7.299E-01	1.272E-03
WNW	0.78	2.616E-03	9.334E-03	9.091E-03	1.468E-01	1.227E-01	1.326E-02	3.705E-01	6.198E-04
NW	0.87	2.851E-03	1.069E-02	1.041E-02	1.105E-01	9.718E-02	8.752E-03	2.995E-01	3.188E-04
NNW	1.26	2.122E-02	3.779E-02	3.857E-02	1.205E-01	1.857E-01	3.144E-03	2.807E-01	2.126E-05
N	1.78	9.692E-03	1.821E-02	1.853E-02	4.477E-02	9.879E-02	3.805E-04	1.038E-01	6.964E-07
NNE	0.80	2.861E-02	4.494E-02	4.618E-02	1.768E-01	1.973E-01	1.403E-02	4.233E-01	5.568E-04
NE	0.38	4.612E-02	9.754E-02	9.462E-02	5.648E-01	4.697E-01	1.071E-01	1.375E+00	1.901E-02
ENE	0.28	6.473E-02	1.422E-01	1.464E-01	8.017E-01	6.288E-01	1.897E-01	1.966E+00	6.045E-02
E	0.25	8.020E-02	1.808E-01	1.838E-01	1.048E+00	8.088E-01	2.572E-01	2.568E+00	9.728E-02
ESE	0.26	1.223E-01	2.530E-01	2.524E-01	1.365E+00	1.071E+00	3.348E-01	3.334E+00	1.021E-01
SE	0.32	1.434E-01	2.838E-01	2.918E-01	1.449E+00	1.182E+00	3.153E-01	3.534E+00	5.447E-02
SSE	0.54	1.024E-01	1.946E-01	2.000E-01	8.424E-01	7.922E-01	1.102E-01	2.043E+00	6.152E-03
S	0.95	6.642E-02	1.215E-01	1.255E-01	4.106E-01	5.188E-01	2.119E-02	9.703E-01	2.528E-04

Table 4.7b 97 percentile D/Q of the annual accumulative frequency for the 16 downwind directions calculated for Xe unclides with supersonic wind data ($u < 0.5$ m/s)

(unit: μrem/MeV.Ci)

Downwind Direction	Distance (km)	131m Xe	133m Xe	133 Xe	135m Xe	135 Xe	137 Xe	138 Xe	139 Xe
SSW	0.85	6.036E-02	1.048E-01	1.077E-01	3.735E-01	4.393E-01	2.414E-02	8.875E-01	3.316E-04
SW	0.56	7.315E-02	1.336E-01	1.377E-01	5.724E-01	5.450E-01	7.126E-02	1.375E+00	2.996E-03
WSW	0.46	8.096E-02	1.326E-01	1.365E-01	6.382E-01	5.642E-01	1.004E-01	1.554E+00	7.185E-03
W	0.69	5.335E-02	8.659E-02	8.915E-02	3.687E-01	3.901E-01	3.484E-02	8.876E-01	1.062E-03
WNW	0.78	3.773E-03	1.348E-02	1.313E-02	1.364E-01	1.239E-01	1.326E-02	3.705E-01	5.169E-04
NW	0.87	2.211E-02	3.613E-02	3.707E-02	1.593E-01	1.704E-01	1.033E-02	3.802E-01	2.608E-04
NNW	1.26	2.638E-02	4.348E-02	4.473E-02	1.321E-01	2.071E-01	3.493E-03	3.077E-01	1.761E-05
N	1.78	6.710E-03	1.261E-02	1.283E-02	3.099E-02	6.839E-02	2.634E-04	7.185E-02	5.919E-07
NNE	0.80	2.776E-02	4.334E-02	4.473E-02	1.729E-01	1.963E-01	1.293E-02	4.120E-01	4.835E-04
NE	0.38	5.213E-02	9.969E-02	1.032E-01	5.325E-01	4.497E-01	1.028E-01	1.302E+00	1.691E-02
ENE	0.28	6.027E-02	1.321E-01	1.361E-01	7.686E-01	6.086E-01	1.771E-01	1.877E+00	5.240E-02
E	0.25	7.549E-02	1.627E-01	1.659E-01	9.127E-01	7.044E-01	2.238E-01	2.234E+00	7.653E-02
ESE	0.26	9.511E-02	1.898E-01	1.952E-01	1.041E+00	8.131E-01	2.499E-01	2.550E+00	7.133E-02
SE	0.32	9.931E-02	1.927E-01	1.982E-01	1.001E+00	8.117E-01	2.123E-01	2.453E+00	3.631E-02
SSE	0.54	8.515E-02	1.656E-01	1.707E-01	7.134E-01	6.862E-01	9.242E-02	1.738E+00	4.197E-03
S	0.95	5.296E-04	1.934E-03	1.883E-03	2.961E-02	2.852E-02	1.968E-03	8.017E-02	1.686E-04

Table 4.8a 97 percentile D/Q of the annual accumulative frequency for the 16 downwind directions calculated for Kr nuclides with propeller wind data

(unit: μrem/MeV.Ci)

Downward Direction	Distance (km)	85m Kr	85 Kr	87 Kr	88 Kr	89 Kr	90 Kr
SSW	0.85	3.096E-01	3.806E-03	1.092E+00	2.693E+00	1.413E-01	2.002E-04
SW	0.56	4.246E-01	5.160E-03	1.546E+00	3.721E+00	5.601E-01	2.974E-03
WSW	0.46	4.132E-01	5.171E-03	1.598E+00	3.852E+00	8.178E-01	8.316E-03
W	0.69	1.978E-01	2.609E-03	7.727E-01	1.924E+00	2.294E-01	7.963E-04
WNW	0.78	6.430E-02	1.323E-03	4.216E-01	1.062E+00	1.012E-01	3.230E-04
NW	0.87	6.055E-02	1.060E-03	3.547E-01	9.601E-01	7.121E-02	1.383E-04
NNW	1.26	1.199E-01	1.616E-03	4.416E-01	1.135E+00	1.562E-02	3.829E-06
N	1.78	6.218E-02	8.851E-04	2.300E-01	6.311E-01	1.405E-03	3.490E-08
NNE	0.80	1.313E-01	1.677E-03	4.894E-01	1.291E+00	9.246E-02	2.799E-04
NE	0.38	3.149E-01	3.929E-03	1.207E+00	2.911E+00	8.447E-01	1.948E-02
ENE	0.28	4.360E-01	5.121E-03	1.607E+00	3.817E+00	1.559E+00	6.820E-02
E	0.25	5.533E-01	6.629E-03	2.075E+00	4.860E+00	2.074E+00	1.137E-01
ESE	0.26	7.458E-01	8.691E-03	2.710E+00	6.397E+00	2.674E+00	1.132E-01
SE	0.32	8.092E-01	9.644E-03	2.986E+00	7.030E+00	2.460E+00	5.444E-02
SSE	0.54	5.448E-01	6.586E-03	1.991E+00	4.795E+00	7.577E-01	5.041E-03
S	0.95	3.471E-01	4.387E-03	1.243E+00	3.097E+00	1.144E-01	9.229E-05

Table 4.8b 97 percentile D/Q of the annual accumulative frequency for the 16 downwind directions calculated for Kr nuclides with supersonic wind data (u < 0.5 m/s)

(unit: μrem/MeV.Ci)

Downward Direction	Distance (km)	85m Kr	85 Kr	87 Kr	88 Kr	89 Kr	90 Kr
SSW	0.85	2.952E-01	3.700E-03	1.064E+00	2.627E+00	1.380E-01	1.490E-04
SW	0.56	3.761E-01	4.555E-03	1.361E+00	3.272E+00	4.885E-01	2.351E-03
WSW	0.46	3.820E-01	4.701E-03	1.437E+00	3.434E+00	7.187E-01	6.628E-03
W	0.69	2.610E-01	3.227E-03	9.545E-01	2.333E+00	2.343E-01	6.560E-04
WNW	0.78	7.398E-02	1.227E-03	4.216E-01	1.108E+00	1.045E-01	2.707E-04
NW	0.87	1.124E-01	1.592E-03	4.604E-01	1.169E+00	6.929E-02	1.132E-04
NNW	1.26	1.337E-01	1.779E-03	4.841E-01	1.244E+00	1.618E-02	3.122E-06
N	1.78	4.305E-02	6.128E-04	1.592E-01	4.369E-01	1.041E-03	3.015E-08
NNE	0.80	1.296E-01	1.650E-03	4.779E-01	1.211E+00	8.017E-02	2.414E-04
NE	0.38	3.053E-01	3.681E-03	1.139E+00	2.725E+00	7.916E-01	1.738E-02
ENE	0.28	4.148E-01	4.966E-03	1.545E+00	3.624E+00	1.429E+00	5.968E-02
E	0.25	4.768E-01	5.716E-03	1.796E+00	4.233E+00	1.821E+00	8.736E-02
ESE	0.26	5.526E-01	6.634E-03	2.074E+00	4.861E+00	1.981E+00	7.947E-02
SE	0.32	5.602E-01	6.637E-03	2.064E+00	4.880E+00	1.640E+00	3.788E-02
SSE	0.54	4.693E-01	5.598E-03	1.698E+00	4.080E+00	6.420E-01	3.271E-03
S	0.95	1.537E-02	3.009E-04	1.027E-01	2.885E-01	2.005E-02	6.157E-05

Table 4.9 The external γ whole body exposures due to the release of Xe and Kr nuclides in a postulated accident calculated using propeller and supersonic wind data

(unit : mrem)

Type	Xe	Kr	Total
Propeller u<0.5 m/s	6.36	6.81	13.17
Supersonic u<0.5 m/s	5.74	6.01	11.75

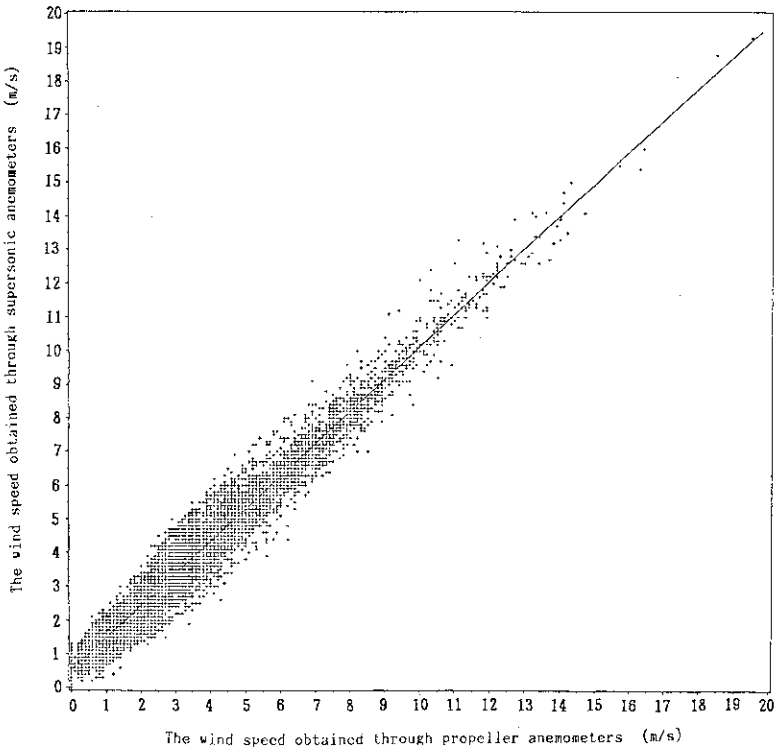

Fig. 2.1 The correlation between the 10m and 40m height hourly average wind speed readings obtained by propeller anemometers and the corresponding wind speed readings obtained by supersonic anemometers.

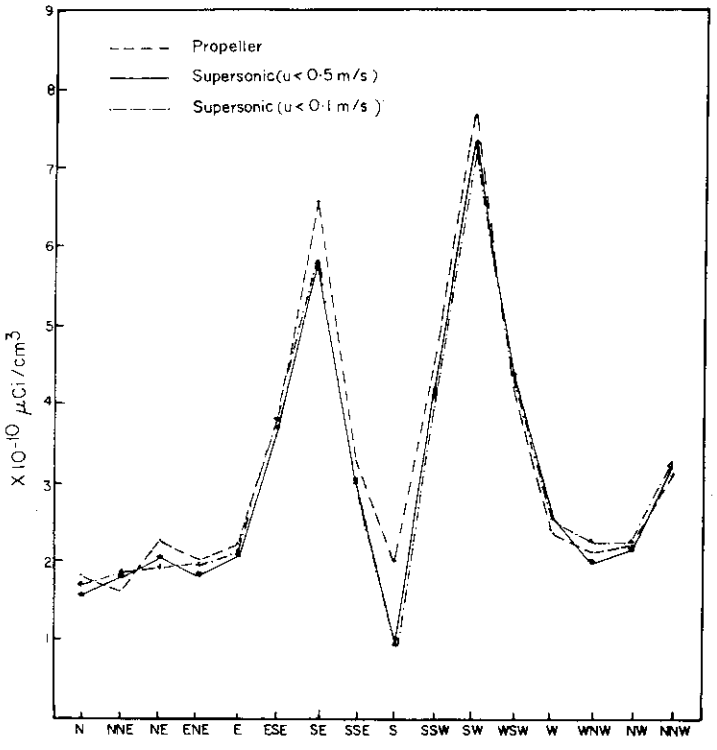

Fig. 3.1 Average air concentration due to continuous releases of radionuclides at 40m stack height calculated at 1 km distance for 16 directions.

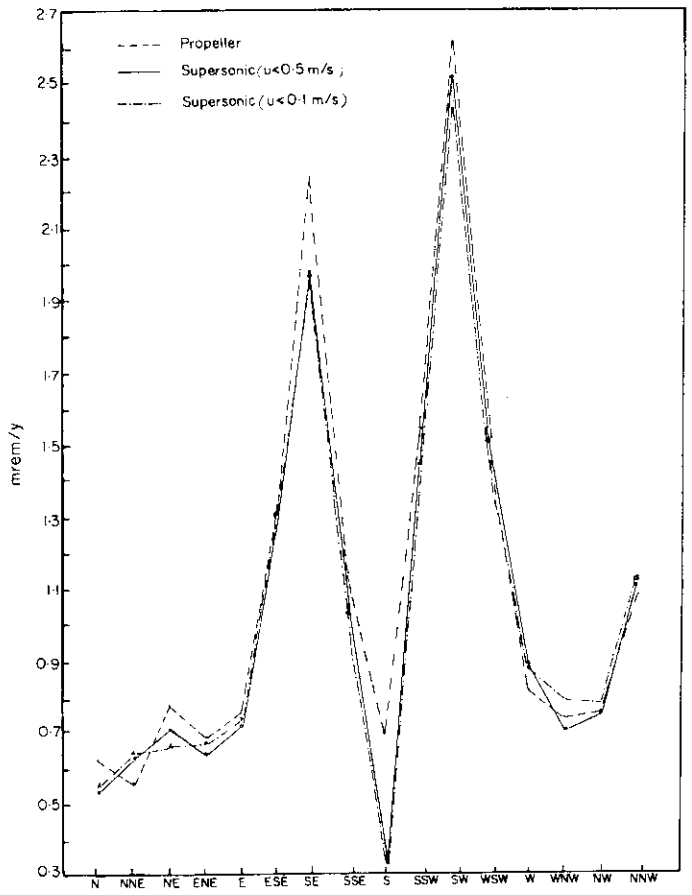

Fig. 3.2 Ground level external γ exposure rate $D_{\gamma S}$ due to continuous releases of radionuclides at 40m stack height calculated at 1 km distance for 16 directions.

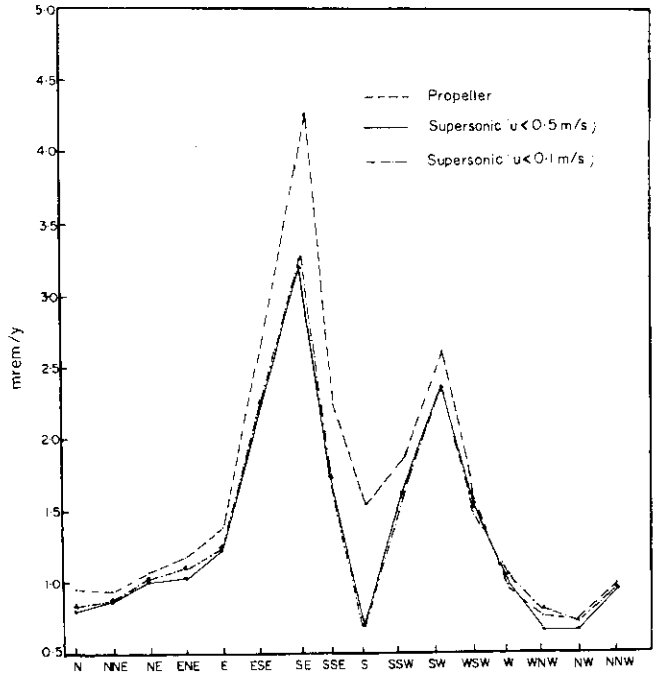

Fig. 3.3 Ground level external γ exposure rate D_{γ} due to the continuous releases of radionuclides at 40m stack height calculated at 1 km distance for 16 directions.

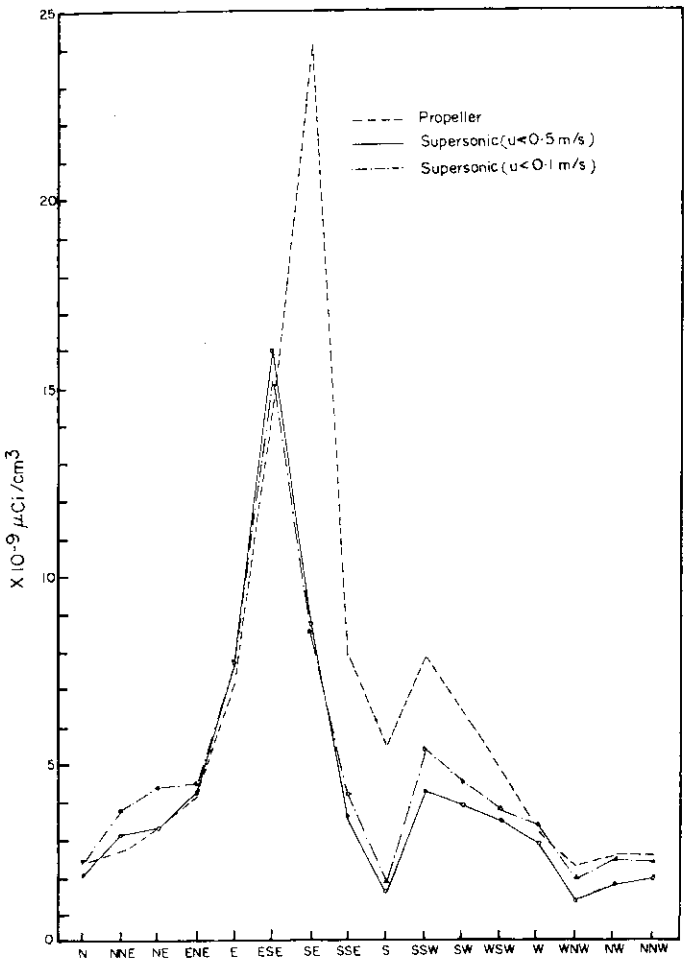

Fig. 3.4 Average air concentration due to continuous releases of radionuclides at 10m stack height calculated at 1 km distance for 16 directions.